Neuro-robotics Paradigm for Intelligent Assistive Technologies

Nicola Vitiello[1], Calogero Maria Oddo[1], Tommaso Lenzi[2], Stefano Roccella[1], Lucia Beccai[3], Fabrizio Vecchi[1], Maria Chiara Carrozza[1], and Paolo Dario[1]

[1] The BioRobotics Institute, Scuola Superiore Sant'Anna, Viale Rinaldo Piaggio, 34, 56025, Pontedera, Pisa, Italy
[2] Northwestern University, Feinberg School of Medicine, Chicago, Illinois, USA
[3] Center for Micro-BioRobotics@SSSA, Istituto Italiano di Tecnologia, Viale Rinaldo Piaggio, 34, 56025, Pontedera, Pisa, Italy

1 Introduction to Neuro-robotics

The *neuro-robotics paradigm* is a design approach, mainly aimed *at the fusion of neuroscience and robotic competences and methods* to design better robots that can act and interact closely with humans, in several application fields: rehabilitation and personal assistance, prosthetics, urban services, surgery, diagnostics, and environment monitoring.

The neuro-robotics design paradigm relies on a strongly co-ordinated, multidisciplinary and interdisciplinary effort which involves three main scientific areas:

- *robotics*, with special reference to bio-mimetic, anthropomorphic systems and bionic components,
- *neuroscience,* with special reference to sensory-motor coordination;
- and *interfacing technology,* with reference to non-invasive and invasive interfaces to the peripheral nervous system (PNS) as well as to non-invasive interfaces to the central nervous system (CNS).

Mostly, the neuro-robotics paradigm applies in the research area of 'human augmentation' through 'hybrid bionic systems'. As suggested by E. Von Gierke, a pioneer of this discipline, the primary goal of *bionics* is "to extend man's physical and intellectual capabilities by prosthetic devices in the most general sense, and to replace man by automata and intelligent machines" (Von Gierke et al., 1970).

Hybrid Bionic Systems (HBSs) can be generically defined as systems that contain both technical (artificial) and biological components. They can include:

- *artificial systems* with *biological elements* or subsystems. In such a case, the biological system is a complementary or supplementary element to the technical system;
- *biological systems* with *artificial elements* or subsystems. The artificial subsystem, e.g. a robotic artefact, is a complementary or supplementary element to the biological system.

S. Mohammed et al. (eds.), *Intelligent Assistive Robots*,
Springer Tracts in Advanced Robotics 106, DOI: 10.1007/978-3-319-12922-8_1

In recent years, many scientific and technological efforts have been devoted to create HBSs that link, via neural interfaces, the human nervous system with electronic and/or robotic artefacts. In general, this research has been carried out with various aims: on the one hand, *to develop systems for restoring motor and sensory functionalities in injured and disabled people*; on the other hand, *for exploring the possibility of augmenting sensory-motor capabilities of humans in general*, not only of disabled people.

Examples of devices for the restoration of lost sensory-motor functions are: neuroprostheses for subjects with neurological disorders, such as those caused by spinal cord injury (SCI) or stroke/head injury (Stein et al., 1992; Popovic and Sinkjaer 2000; Lauer et al., 2000); robotic devices like the LOPES, Lokomat, HAL5, ReWalk, EKSO (Craelius, 2002; Veneman et al., 2006; Jezernik et al., 2003; Kawamoto and Sankai, 2005; Esquenazi et al., 2012; Mertz, 2012), active exoskeletons which can augment or replace muscular functions of the lower limbs, for example to assist motor-impaired individuals; or powered upper- and lower-limb prostheses (Edin et al., 2008; Carrozza et al., 2006; Velliste et al., 2008; Sup et al., 2008; Hargroveet al., 2013).

As for sensory functionalities, important results have been achieved in restoring hearing and sight capabilities. Some improvements in auditory performance of people with hearing loss can be obtained with cochlear implants (Simmons et al., 1965; Blume, 1999; Loizou, 1999; Spelman, 1999; Marsot-Dupuch et al., 2001). Retinal implants can be realized in the attempt to regain lost visual functionality (Eiber et al., 2013).

Examples of HBSs which aimed at augmenting capabilities of able-bodied persons were developed within the framework of the DARPA program called Exoskeletons for Human Performance Augmentation (EHPA). The goal of this program was to "increase the capabilities of ground soldiers beyond that of a human" and led to the development of three exoskeletons: the Berkeley Exoskeleton (BLEEX), the MIT Exoskeleton and SARCOS (Dollar and Herr, 2008).

2 The Strategic Alliance between Robotics and Neuroscience

George Bekey (2005) defined a robot as a "machine that senses, thinks, and acts", and which is "embodied and situated in the real world". Robots have physical dimensions, and they can exert forces on other objects. Robots are also subject to the world's physical laws, they have mass and inertia, their moving parts encounter friction and hence produce heat, measurements are corrupted by noise, and parts break. Robots also contain computers, which provide them with ever increasing speed and power for both signal processing and cognitive functions. In other terms, Robots "are an imitation of life". They "appear to move intelligently, they avoid obstacles, they interact with one another, and they accomplish tasks". Roboticists have the goal of enabling robots "to perform these and other actions".

Under this perspective, a grand challenge for robotics is to develop new robots with the capability to work for, and to interact effectively and friendly with, human beings. In order to achieve this goal robotics needs not only *new technology*, but also

more science. Investigating and taking inspiration from biological models (in particular from the human model) to design new robots is an approach increasingly adopted by the robotics research community. Neuroscience (whose goal is "to understand the mind, how we perceive, move, think and remember", as Eric R. Kandel, James H. Schwarts and Thomas M. Jessell pointed out in the book "Principles of Neural Science") is an excellent example of a scientific discipline that could provide knowledge, models and methodological tools for advancing robotics progress.

Starting from the robotics challenges and the neuroscience potentialities, the neuro-robotics design paradigm, which fuses robotics and neuroscience methodologies, tools and scientific knowledge, aims to be beneficial for the progress of both robotics and neuroscience. Indeed, on one hand, the neuro-robotics paradigm aims to enhance the development of *a new generation of robotic systems*, such as advanced HBSs for human assistance and augmentation. On the other hand, neuro-robotics aims at achieving new neural-scientific findings.

Under the neuro-robotics umbrella, roboticists and neuroscientists have three main "opportunities" for an effective cooperation.

One opportunity is that roboticists can provide advanced platforms to be used as a *tool for supporting neuroscience investigations.* For instance, the robotic device can be used either to measure and record specific parameters of neuroscientific interest, such as the position and velocity of the human hand (Burdet et al., 2000) or the impendence of the human arm during reaching movements (Gomi and Kawato, 1997), or to interact with a subject to analyze his/her responses to a specific external stimulus, such as the response to a tactile stimulus on the fingertip (Andrè et al., 2009), or the effect of a given force disturbance on the hand trajectory (Burdet et al., 2001). In both the above cases, the object of the scientific investigation is barely neuroscience-driven, e.g. the *behaviour of human within a certain scenario.* This is maybe the simplest way neuroscience and robotics can interact and cooperate.

Another possible opportunity is the development of *robotic models* (physical platforms) to test and validate neuroscience theories. In this case, the validation of a neuroscientific model or hypothesis is conducted through the experimental activities performed by means of a robotic model. Examples of robotic models are: the *salamander robot driven by a spinal cord model*, for the investigation of how a primitive neural circuit for swimming can be extended, by phylogenetically more recent limb oscillatory centers, to explain the ability of salamanders to switch between swimming and walking (Ijspeert et al., 2007); the lamprey-like robot (Dario et al., 2006; Stefanini et al, 2006; Manfredi et al., 2013) for the investigation of motion control strategies based on central pattern generators in lampreys (Ekeberg et al., 1995; Grillner et al., 1995; Grillner, 1985); the brachiation robot, aimed at the investigation of gorilla's brachiation (Fukuda and Soito, 1996); the snake robot (Hirose and Morishima, 1990) for the investigating of snake's locomotion. Other interesting examples of robotic models are related to the investigation of human behaviour, such as robotic arms and hands used to support the analysis of human arm motor control, visual-motor coordination and hand grasping and writing tasks. Among many, Schaal and Sternad used an anthropomorphic robotic arm for the investigation of mechanisms of rhythmic movements generation (Sternad and Schaal, 1999; Schaal and Sternad, 2001); Potkonjak

and colleagues used a 5-degree-of-freedom (DOF) anthropomorphic robotic arm to investigate the human multi-joint coordination in the demanding task of hand writing (Potkonjal et al., 1998); Zollo and colleagues used a platform consisting of the anthropomorphic robotic arm Dexter, of a robotic hand and of a visually-capable head to investigate different models of high-level sensory motor control (Zollo et al., 2008); Edin, Carrozza and their colleagues employed a highly sensorized artificial robotic hand to investigate the grasp-and-lift task (Edin et al., 2008; Carrozza et al., 2006). Using robotic models for neuroscience investigation is a key point of the neuro-robotics paradigm, which can lead to the development of new technologies (the ones necessary to develop the robotic models), and more generally to the development of a new generation of robotic artefacts.

Finally, the third way neuroscience and robotics can cooperate is when robotics takes inspiration from neuroscience for the development of a new robot, or a new human-robot interfacing system. In this case robotics is neither just a tool or a model: robotics benefits of neural science to generate artefacts that are revolutionary and pioneering. Examples of input from neuroscience are: *motion control theories, sensory-motor coordination frameworks, behavioural models and learning strategies.* This scenario is much likely the most interesting: it allows to imagine that *bio-inspiration* goes beyond the *usual biomimetic morphology*, and lead to new control strategies for *motion control and human-robot interfacing*.

It is worth noting that neuroscience and robotics can cooperate in a wide framework which is not limited to only one of the above opportunities. Indeed, rather than a limiting taxonomy, the description of these three opportunities represent a description of the potentiality of the strategic alliance between robotics and neuroscience.

3 Neuro-robotics is a Development Engine for New Assistive Devices

By moving from the potentialities of the neuroscience-robotics collaboration - in this chapter - we review the following three research activities (case studies) carried out at The BioRobotics Institute of Scuola Superiore Sant'Anna in the past decade.

- Case-study #1: development of *a robotic tactile stimulator for human active and passive touch studies*, to be used as precise *tool* to stimulate the human finger pad under repetitive and controlled stimulation conditions.
- Case-study #2: development of NEURARM, *a new robotic model of the human arm* which mimicked the dynamic properties (i.e. link masses, and joint inertia, damping and stiffness) of the human upper limb.
- Case-study #3: development of NEUROExos, an *elbow robotic exoskeleton with a biomimetic antagonistic actuation* capable of changing its joint output impedance, in a human-like fashion.

4 A Neuro-robotic Tactile Stimulation Platform to Enable Human and Artificial Touch Studies

4.1 Motivation, Design Requirements and State-of-Art Analysis

Passive- and active- touch are the main experimental paradigms used in the literature to study the neuronal mechanisms of the sense of touch in the human hand.

Various definitions of the passive- and active- paradigms are actually possible, and a simple one involves considerations on the energy flow associated to the dynamic phases of the tactile experience (Prescott, 2011). With such a definition, similarly to passive measurement instruments, in dynamic passive-touch the (kinetic) energy required to apply the relative motion between the sensory system and the tactile surface is provided via the surface under test. Conversely, in active-touch protocols the (kinetic) energy to achieve the dynamic tactile stimulation condition is provided by an actuated mechanism closely integrated with the (human or artificial) sensory system.

A possible application of such definition to dynamic-touch studies (either passive- or active-) results in the core of the tactile stimulation sequence being characterized by a tangential relative motion between the fingerpad and the (textured) surface. Therefore, in such case the difference between passive- and active- is in the body (i.e., fingertip or tactile stimulus) which actually moves with respect to a chosen reference frame. The relative motion can be obtained by sliding the tactile stimulus while the fingertip is still (passive- dynamic-touch) (Yoshioka et al., 2001), or by exploration via the finger (active- dynamic-touch) while the tactile stimulus is static (Lawrence et al., 2007).

While considering the deformation of skin tissues, established findings showed that passive- and active- passive protocols are equivalent (e.g., up to 4 N in Birznieks et al., 2001). In addition, one may wonder whether this is the same at perceptual level, considering that in passive-touch there is a lack of voluntary movement, while in active-touch the percept may be integrated by kinesthetic afferent sensory feedback or by efference copy associated to motion dynamics of the body part. However, with respect to this particular point, a dedicated study on the perception of roughness (Lederman, 1981) excluded relevant differences between passive- and active- touch protocols.

In both human and artificial passive-touch studies, the presentation of tactile stimuli should be replicated several times repeatably in the same conditions to infer models based on statistical analysis of acquired data (Johansson and Birznieks, 2004); also, the passive-stimulation operation should avoid to introduce spurious information by the system delivering the tactile surfaces.

To achieve standardization and repeatability, the passive-touch approach requires a robotic stimulator that enables detailed analyses of receptor response through controlled variation of stimulation parameters (e.g. stimulus spatial coarseness, materials and tribological properties) to make comparisons between sessions or participants, or to average over a large number of replications.

There are a number of particular requirements in the design of such a robotic tactile stimulation device.

First, to allow repeatable experiments with standardized conditions, accuracy and precision in the control of stimulation parameters, such as the contact force and the sliding velocity profile, is required.

Second, the device must guarantee a range of forces and movement velocities covering those that would naturally be used by humans in the exploration of textures, while both normal and tangential forces need to be recorded as they are fundamental quantities for human touch investigation. Studies on discriminative touch (Johnson and Yoshioka, 2001; Jones and Lederman, 2006) suggested:

- for the indentation force a range of at least 100 mN–5 N, with a control accuracy of about 5% of the reference force and sensing resolution within a few mN;
- 100 mm of stroke along the sliding direction and velocities up to 150 mm/s with μm position sensing resolution and steady state control accuracy.

Such requirements apply to both artificial and human touch studies but the latter ones present additional constraints due to the particular neurophysiological experimental methods while dealing with the biological system.

The third challenging requirement, given that some classes of tactile receptors are highly sensitive to vibration up to 400 Hz or more (Connor and Johnson, 1992), is in developing a stimulator that could get into contact with the human finger free from any spurious vibration that could interfere with the encoding of tactile stimuli.

Fourth, electrophysiological methods such as microneurography and EEG involve recording of signals in the μV range, and electromagnetic interference from the robotic system has to be minimized.

Fifth, these experiments can require the participant to sit in a natural position and to remain relaxed for hours. Hence, the subject's comfort puts stringent demands on the mounting of the device and on the control laws of each DoF so that it can be adapted in 3D space to the position of the subject's arm, hand and finger (Birznieks et al., 2001).

Finally, the programming operation by the experimenter to implement the targeted protocols has to be simple and flexible, and upgradeability of the platform should be possible.

The reviewed previous works span from platforms with flat or curve extended textured stimuli for studying the application of ridged or dotted surfaces to the fingerpad, to other devices with wide or pointed probes, to pinned stimulators for applying spatio-temporal indentation profiles with an array of contact locations. Some neurophysiological studies addressed the response of single afferents to the applied stimuli, while others took into account population of mechanoreceptors. Nevertheless, one of the major limitations of most of reviewed platforms is that they were developed for touch experiments in monkeys rather than humans, then presenting less demanding requirements since higher level of invasiveness is tolerated in animal model studies (Goodwin and Morley, 1987; LaMotte et al., 1998).

A considerable input was given in the 70's by the availability of digital controllers (Looft and Williams, 1979) which enabled the design of mechatronic platforms with customizable motion profiles to address specific experimental paradigms. This is confirmed by the fact that in the 80's a few platforms integrated complex mechanisms (Goodwin et al., 1985) for tuning the desired stimulation parameters. Furthermore, the analog circuitry was reduced as much as possible, remaining between the sensors and the controller only, and between the controller and the actuators or, at most, for implementing low-level force (or position) servo control (Byrne, 1975; Looft and Williams, 1979; LaMotte et al., 1983). As a matter of fact, almost all the reported tactile platforms employed digital processors for data storage at least, and for the generation of force and position references. In contrast to the almost standardized architecture for the control electronics, a greater variability could be found between the core mechanisms of the reported systems.

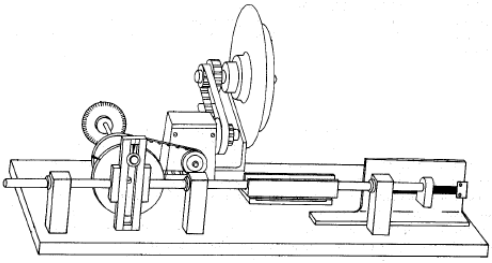

Fig. 1. From Goodwin et al. (Journal of Neuroscience Methods 1985). A schematic diagram of the scotch yolk stimulator (reprinted with permission from Elsevier).

In the class of devices that were built to study the neural coding and perception of texture, Goodwin and colleagues (1985) used a scotch yolk driven by a DC motor which rotated at constant speed for producing a sinusoidal motion (Fig. 1). The motion control was completely in open-loop, relying on the non-backdrivability of the mechanism in spite of subject-machine interaction. The advanced stimulator shown by LaMotte and colleagues (1983) controlled the sliding motion and the indentation position or load force of a selectable surface which, in turn, contacted and stroked the skin of the fingerpad in passive-touch studies. The stimulus could be selected among eight flat plates carrying textured surfaces. The user could select the motion profiles, allowing the definition of the horizontal and vertical displacements or the load force, and the displacement velocities, however it was very bulky to be easily oriented in 3D space and it relied on the early digital electronics available at the time.

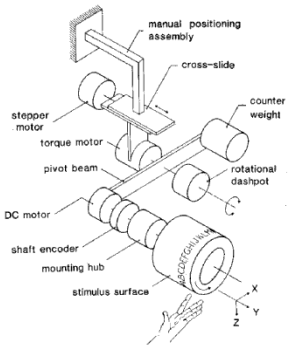

Fig. 2. From Johnson and Phillips (Journal of Neuroscience Methods 1988). An example system belonging to the class of rotating drum stimulators (reprinted with permission from Elsevier).

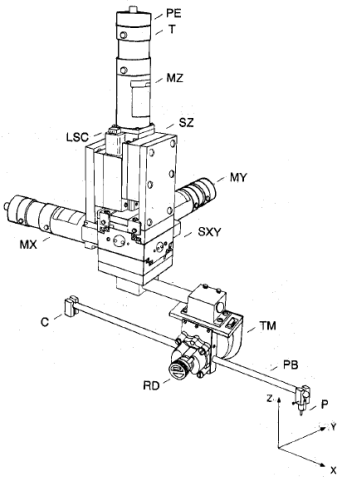

Fig. 3. From Romo et al. (Journal of Neuroscience Methods 1993). Design of the scanning probe stimulator suitable for indenting and sliding punctuated stimuli to the fingerpad (reprinted with permission from Elsevier).

A number of groups (Darian-Smith and Oke, 1980; Johnson and Phillips, 1988; Romo et al., 1993; Radwin et al., 1993; Wheat et al., 2004) utilized beams for the application of stimuli to the subjects. The devices shown by Darian-Smith and Oke (1980) and by Johnson and Phillips (1988), the latter being an improved version of the stimulator described by Johnson and Lamb (1981), had a rotating drum with embossed patterns mounted at one end of a pivot beam (Fig. 2). A major difference between the two rotating drum platforms regards the motion along the indentation direction. Darian-Smith and Oke (1980) chose an electronically controlled solenoid for enabling the counterweight to apply the desired force, while Johnson and Phillips (1988) used a torque motor driven in open loop mode for regulating the interaction

force. Both the rotating drums platforms used dampers, also applied to other devices (Romo et al., 1993; Wheat et al, 2004; Oddo et al., Mechatronics 2011), for minimizing any transient increase in the contact force at the onset of the stimulation, or to reduce the propagation of vibrations to the human subject (Fig. 3).

Another class of tactile stimulators is represented by pinned systems (Bliss et al., 1970; Gardner and Palmer, 1989; Killebrew et al., 2007). A noticeable number of such devices has been reported in literature (wideband devices were shown by Summers and Chanter, 2002 and by Kyung et al., 2006), being of great interest for pointed and distributed stimulation of the fingerpad stimulation, also allowing flexible experimental paradigms with a variety of spatio-temporal stimulation profiles (Vidal-Verdú and Hafez, 2007).

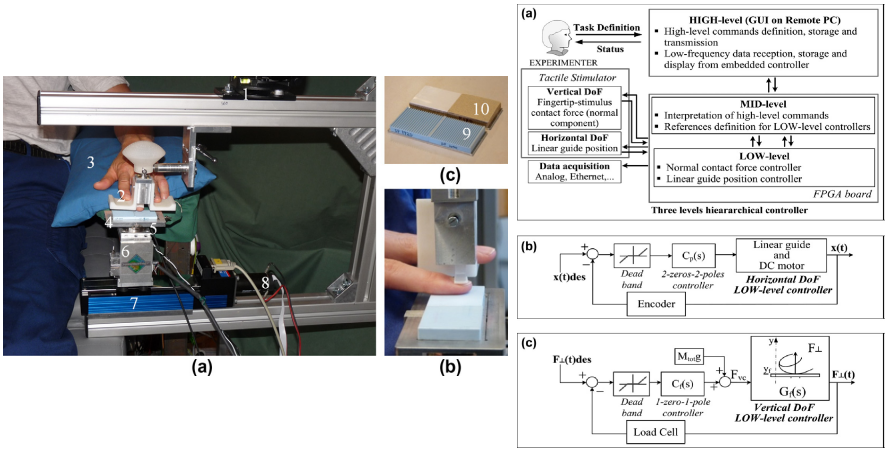

Fig. 4. Mechatronic tactile stimulation platform by Oddo et al. (Mechatronics, 2011). Left: (a) Experimental set-up during microneurography: frame hold by spherical joint (1), hand-finger support system (2), vacuum cast for arm support (3), carrier for stimuli (4), load cell (5), voice-coil actuator assembly for indentation of stimuli (6), linear guide for tangential sliding of stimuli (7), DC motor with encoder (8). (b) Fingerpad-stimulus interface with finger fixation system and free fingers support. (c) Examples of the used stimuli glued to a changeable aluminum plate: a couple of ridged stimuli (9), smooth plastic and rough sandpaper (10). Right: (a) Overview of the Dynamic Platform hierarchical controller. (b) Block diagram of the LOW-level closed-loop position controller along the sliding direction. (c) Block diagram of the LOW-level closed-loop force controller along the indentation direction (reprinted with permission from Elsevier).

4.2 Overview of the Robotic Platform

A 2-DOF mechatronic system (Oddo et. al, Mechatronics 2011) was dedicatedly developed to enable passive-touch protocols that are the core of this case study on neuro-robotic platforms for investigating the sense of touch. The developed platform fulfils all the requirements detailed above for passive-touch tactile stimulation and was replicated in five exemplars delivered to European research groups within the FP7 Nanobiotouch project, with customizations for electrophysiological,

psychophysical, and artificial touch studies and for tribological experiments on different tactile surfaces as well. It can be used to perform neurophysiological studies in humans with techniques such as microneurography and EEG (Beckmann et al., 2009) even in combination with psychophysical experimental paradigms. Also, it is suitable for tribological and artificial touch studies as well.

The platform could indent and slide sequences of textured stimuli (lodged in 77 mm x 32 mm changeable plates) to the fingerpad with feedback-controlled normal contact force and parametric sliding trajectories while recording (Smith et al., 2002; Libouton et al., 2010) the normal and tangential forces at finger-stimulus interface; a voice-coil actuator (NCC05-18-060-2X, H2W Tech.) applied the indentation force with a 12.7 mm stroke, and a linear guide (LTP 60.180.0804-02, SKF Multitec) driven by a DC motor (RE35, Maxon Motors) applied the sliding motion through a 4 mm pitch ball bearing screw, allowing a maximum velocity of 300 mm/s and a stroke of 110 mm. Linear Current Amplifier Modules (LCAM, Quanser), guaranteeing very low electromagnetic interference, were chosen for driving the actuators. Switching power devices were avoided since the typical (10–50 kHz) range for PWM carrier frequency is higher than half the microneurography sampling rate, but just outside the cutoff frequency of the bandpass filter preceding the sampling block. Hence, even introducing shielding techniques, a residual slight coupling between the PWM carrier frequency and μV range microneurography data could have been aliased at significant low frequencies, affecting the band of interest.

The robotic system has been devised with an open design approach since it is simple to command via a graphical user interface and is upgradable thanks to the FPGA control electronics. This design choice represented an advancement with respect to state of the art systems coherently with the trend showed in the literature of mechatronic tactile stimulators, which used digital controllers (Looft and Williams, 1979) for avoiding to integrate complex mechanisms such as in the scotch yolk stimulator (Goodwin et al., 1985) and reducing as much as possible the analog circuitry (LaMotte et al., 1983; Byrne et al., 1975; Schneider et al., 1995). Despite this design solution is promising, only a few mechatronic tactile stimulators were based on FPGA control electronics at the time of the platform development (Wagner et al., 2002; Pasquero et al., 2007).

For the platform presented by Oddo and colleagues (Mechatronics, 2011), this choice was operated for two main reasons: i) to allow future upgradeability of the architecture of control electronics (e.g. by instantiating on the same FPGA a number of additional parallel soft-core processors, peripherals, custom digital hardware modules, etc.); ii) to achieve, via hardware-software codesign, a multi-layered hierarchical controller (Fig. 4-right) allowing low-level parallel (Astarloa et al., 2009) scheduling of periodic routines implementing the motion control laws and of interruptions managing the communication (commands and platform data) functions. Therefore, the multi-layered hierarchical control architecture partitioned the tasks between a general purpose PC and the embedded FPGA hardware-programmable logics, which was interfaced to the sensors and power current drivers of the platform (Fig. 4-right a).

The HIGH-level layer ran a Graphical User Interface (GUI) to generate, save, load or execute buffers of HIGH-level commands and for displaying the received platform data. The MID-level layer was in charge of interpreting HIGH-level commands, of point-to-point trajectory generation for the linear guide LOW-level controller, of force target generation for the voice coil LOW-level controller, and of transmitting

the platform variables to the GUI for display purposes and to the acquisition systems for electrophysiological or artificial touch experiments.

The dimensioning of the 2-DOF LOW-level control laws took into account the mechanical characteristics of the fingertip (Serina et al., 1997; Pawluk and Howe, 1999; Nakazawa et al., 2000); both the controllers were in closed loop with integrator to reject disturbances (e.g. variable friction) or modifications of the boundary conditions (e.g. the inclination of the platform in 3D space for adapting it to the position of the subject during electrophysiological recordings); also, they had ad hoc dead bands (Fig. 4-right b) to prevent any steady-state vibration (Iskakov et al., 2007).

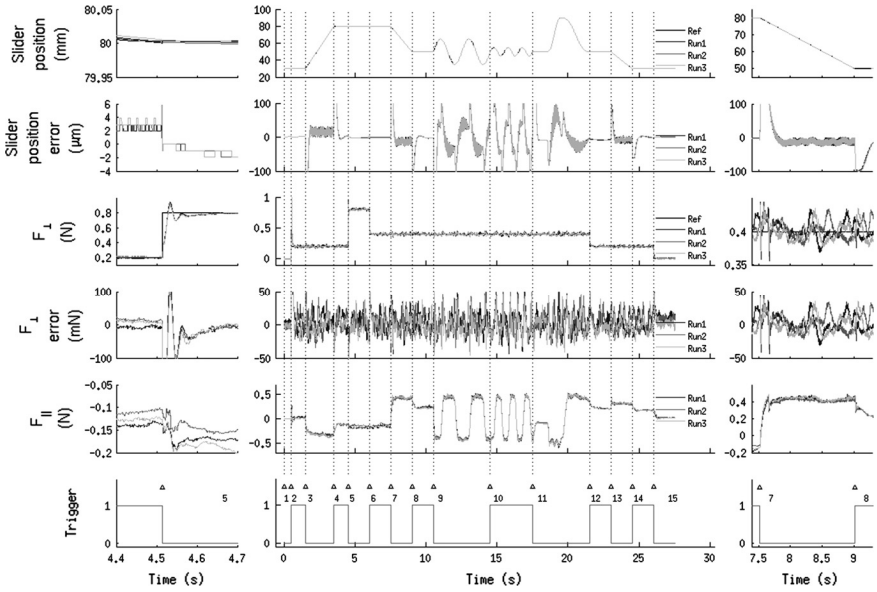

Fig. 5. From Oddo et al. (Mechatronics 2011). Sample protocols that can be implemented with the mechatronic platform. Three runs acquired at 5 kHz through Ethernet digital transmission, of the same sequence of commands are superimposed to show high repeatability. The plots represent, from the top: position of the translational slider (target and actual), error in tracking the reference slider position, indentation force at finger-stimulus interface (target and actual), error in tracking the reference indentation force, tangential force component along the direction of the sliding motion, Boolean channel switching each time a new high-level command is executed. Phases 2 and 15, at the beginning and at the end of the protocol, are the loading and unloading of the smooth aluminum stimulus to the finger. In phase 3 the stimulus is stroked for 50mm at 25 mm/s and normal contact force at 200 mN; phases 5 and 6 are normal contact force steps from 200 mN to 800 mN and then to 400 mN; from phase 7 to phase 11 the normal contact force is held at 400 mN, while the stimulus is stroked for 30 mm at constant speed of 20 mm/s (phase 7), while two (phase 9, 15 mm amplitude at 0.5 Hz) or three (phase 10, 5 mm amplitude at 1 Hz) sine waves are executed, or while a fifth order polynomial trajectory is followed (phase 11). Phase 13 is a position ramp from 50 mm to 30 mm in 1.5 s and normal contact force set to 200 mN. The left inset shows a zoom on the transitory between phase 4 and phase 5. The right inset shows a zoom on dynamic phase 7 (reprinted with permission from Elsevier).

4.3 Experimental Evaluation of the Robotic Platform

Traditional indices (tracking error along the 2 DOFs and confidence intervals to evaluate repeatability) were calculated for assessing the controllers of the 2 DOFs over repeated tactile stimulation runs. Such quantitative indexes confirmed adequate control performances (example protocols are shown in Fig. 5): the reference slider position is tracked with an error lower than 28 μm for ramps (phases 3, 7 and 13 in Fig. 5); reference sine waves (phases 9 and 10) having peak velocities up to 47.1 mm/s are followed with error lower than 68 μm; and 5th order polynomial trajectories (phase 11) present a Tracking Error lower than 43 μm. As regards the regulation of the indentation force, all the calculated parameters showed absolute Tracking Error lower than 20 mN, while the normalized error was comprised between 1.6% and 6.6%. As a further relevant result, the extremely reduced values of the confidence intervals (typically in the order of few permille points of the reference target) confirm that the developed mechatronic platform guarantees excellent repeatability in the presentation of tactile stimuli (Oddo et al., 2011).

This achievement is fundamental in touch studies: even if the tracking of the reference curves may get relatively worse in certain conditions, the actual trajectories under feedback control are almost coincident among different runs.

Apart for the particular design choices and results for traditional robotic assessment, the research work presented by Oddo and colleagues (Mechatronics 2011) also provided neuro-robotic methodological contributions on the possibility to use the human mechanoreceptors as instrumental sensors, to assess platform compatibility with the exacting demands of electrophysiological methods, specifically the lack of electromagnetic interference and absence of spurious vibrations.

The lack of significant electromagnetic interference coupling with the electrode for microneurography due to the platform was investigated by means of analysis of neural recordings from a SAI unit (left index finger), under three experimental conditions: i) Manual Stimulation (MS)-mode: while the platform was not actuated, the experimenter manually stimulated the finger of the subject (test subject) from which neural data was recorded; ii) Closed Loop (CL)-mode: a 1600 μm periodic ridged stimulus was indented and scanned across the fingertip of a second subject (control subject), in close proximity to the fingertip of the test subject (from which neural data was recorded), with 500 mN feedback controlled contact force, sliding distance of 20 mm and velocity set to 20 mm/s; iii) Open Loop (OL)-mode: to double check whether or not the time varying driving current (related to the indentation DoF actuator in feedback force control) affected the microneurography results, the same protocol of point ii) was operated apart for the fact that the indentation was in open loop by supplying a constant current to the voice-coil actuator, resulting in a normal contact force of about 750 mN before the onset of stimulus sliding motion. Noise amplitude distribution was evaluated in the three experimental conditions described above.

No relevant noise pickup was observed in the raw nerve signals (top plots of Fig. 6-right) recorded during platform movement or when the force control was engaged, as an effect of the selected linear power drivers for the actuators instead of switching ones. Fig. 6 depicts neural data from a SAI unit of the test subject in the

three MS-mode, CL-mode and OL-mode experimental conditions detailed above. Neural spikes are identified in MS-mode and marked with dots, corresponding to the phases during which the finger of the test subject was manually probed. The spike template applied for spike sorting in MS-mode was then used to evaluate whether or not neural spikes were elicited under the two other stimulation conditions due to electromagnetic interference by the platform (since the fingertip of the test subject was not mechanically stimulated in CL-mode and OL-mode, and a SAI unit is expected to be silent in that condition). Noticeably, no spikes could be identified in both the CL-mode and OL-mode, confirming that the platform did not induce vibrations resulting in spurious neural firing. As one could expect, the mechatronic platform had an effect in the background neural noise, confirmed by the higher amplitude of the CL-mode and OL-mode traces if compared to the spike-free regions of the MS-mode one. However, the overlap of the traces shows that the increase in noise was not enough to mask the spikes occurring while manually probing (MS-mode) the fingertip of the test subject.

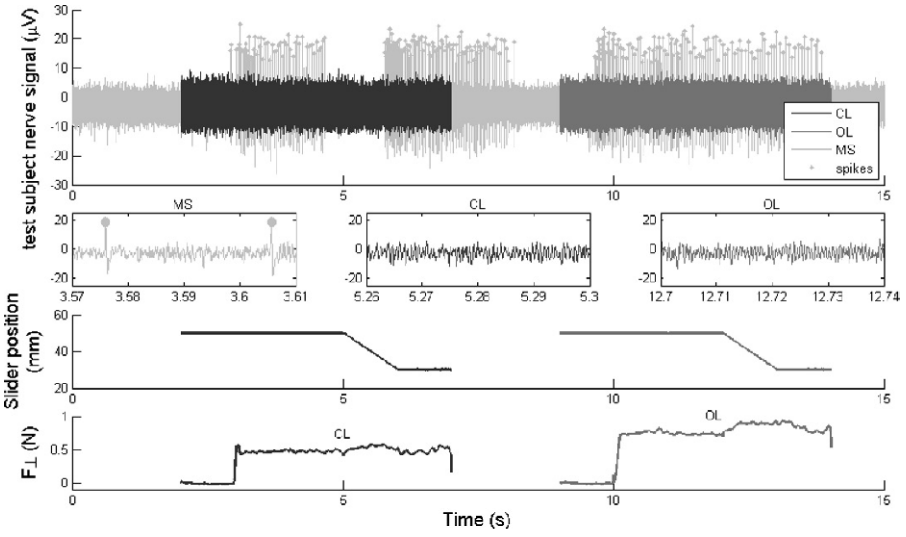

Fig. 6. From Oddo et al. (Mechatronics 2011). Neural recordings under the three MS-mode, CL-mode and OL-mode experimental conditions are depicted in the top plot for assessment of platform electromagnetic compatibility with the microneurographic technique. Left to right, the insets in the second row from the top show zooms on neural data recorded from the test subject with MS-mode, CL-mode and OL-mode. The position of the translational slider and the normal component of the indentation force are shown as well under both the CL-mode and OL-mode experiments (reprinted with permission from Elsevier).

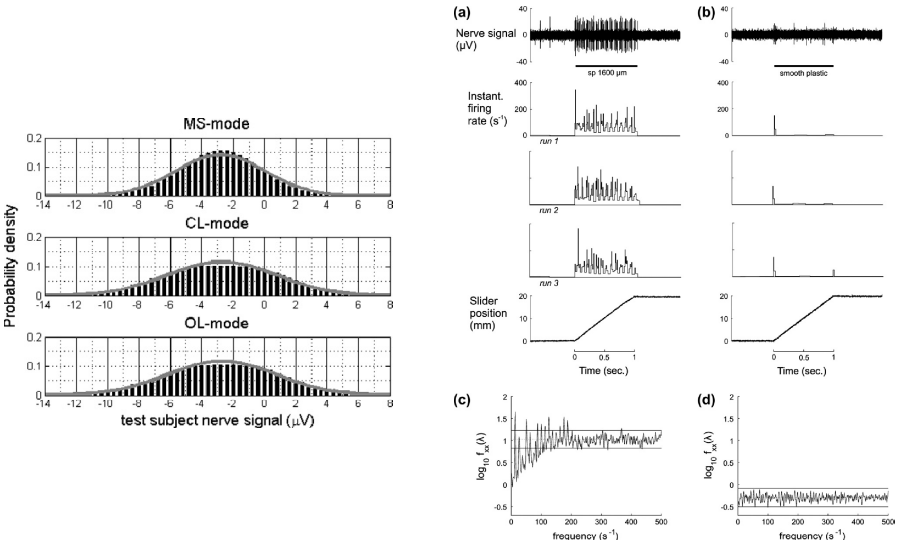

Fig. 7. From Oddo et al. (Mechatronics 2011). Left: Statistical neural noise analysis for each of the three MS-mode, CL-mode and OL-mode stimulation conditions. The probability that the neural signal belongs to a bin (width set to 0.4 lV) is evaluated based on amplitude levels experimentally occurring in 38 s of data at 12.8 kHz. The solid line shows Gaussian fitting of noise probability density. Right: Microneurographic recording from a RA (Meissner) tactile afferent unit. (a) Stimulation with a ridged grating. Records from top, recorded nerve signal, instantaneous rate of nerve discharges during three repeated runs of the same stimulus, slider position. (b) Stimulation with a smooth plastic surface on the same unit, records as in A. (c) Spectrum of nerve discharge during ridged grating stimulation. Solid lines show $p < 0.01$ confidence limits. (d) Spectrum for a smooth surface as in C (reprinted with permission from Elsevier).

A statistical noise analysis is presented in Fig. 7-left for each of the three MS, CL and OL stimulation conditions, where the probability that the neural signal belongs to a bin (width set to 0.4 μV) is evaluated based on amplitude levels experimentally occurring in 38 s of data at 12.8 kHz. A Gaussian fitting is shown as well in Fig. 7-left: platform activation causes a non-relevant increase in noise standard deviation from 2.82 μV (MS-mode) to 3.43 μV (OL-mode) and 3.48 μV (MS-mode), and had almost no effect in its mean value.

To directly assess the presence of biologically significant vibrations introduced by the platform, the spectra resulting from the point processes of identified neural spikes were calculated considering the firing of RA units during indentation and sliding motion of a smooth polypropylene plastic surface, in comparison to that occurring with periodic gratings having spatial period between 280 μm and 1920 μm.

As shown in Fig. 7-right b depicting a single RA afferent, after the expected short burst of impulses at the start of motion, this unit fired only sporadic impulses. The spectral signature of the firing for all the data from the same RA unit is shown in Fig. 7-right c for 1600 μm spatial period grating, meaningfully depicting the modulation of firing at the expected fundamental frequency (i.e. the ratio between the sliding velocity and the spatial period of the presented surface) of 12.5 Hz at a sliding

velocity of 20 mm/s, as well as significant modulation at harmonics up to 200 Hz. Therefore, the spatial period of the grating was revealed as a modulation of firing frequency as the ridges of the surface were sliding across the receptive field of the RA unit, confirming the high sensitivity in encoding the mechanical characteristics of the stimulating surface in this unit. In the frequency domain, the spectrum for all the data from stimulation with a smooth plastic surface in the same unit reveals no periodic firing or pickup of vibrations (Fig. 7-right d). To succeed in this objective, a relevant design choice was the introduction of custom dead bands (Fig. 4-right b and c) which allowed errors lower than specific thresholds to occur, thus avoiding vibrations produced by continuous sub-threshold error-correction control actions.

Human microneurography recordings also confirmed excellent repeatability (Fig. 7-right a), being mainly a consequence of the intrinsically reduced jitter in the scheduling of periodic control tasks by the implemented hierarchical control architecture (particularly, the hardware programmable FPGA logics for the embedded controller). Similar results were obtained in all recorded afferents.

The dedicated design of the platform allowed to implement a wide variety of passive- (Oddo et al., Sensors 2009; Oddo et al., IEEE RoBio 2009; Oddo et al., Sensors 2009; Muhammad et al., MNE 2011; Oddo et al., IEEE TRo 2011; Spigler et al., 2012) and active- (Oddo et al., IEEE TRo 2011) protocols in artificial touch studies, also supported by parallel human touch outcomes via the microneurographic technique (Oddo et al., Sensors 2011). Such studies are now contributing towards a more complete understanding of the human sense of touch and the implementation of an artificial sense and its interfacing with natural neural afferents in amputees.

5 NEURARM: A Robotic Model of the Human Arm

5.1 Background

Experiments addressing questions about how humans adapt their upper-limb impedance have been tested extensively in human and animal subjects, primarily by applying mechanical perturbations (impulses, vibrations, etc.) to the limb during natural movements and observing the corrective responses of the limb (Burdet et al., 2001). These methods have provided a wealth of insight into how the central nervous system (CNS) controls the mechanical behaviour of the limb, however they suffer from the fact that the applied perturbations may themselves change the stiffness characteristics of the arm. A possible way to overcome the measurement artefact problem consists of simulating the human arm movements using mathematical models describing the behavior of the muscle-skeletal system (Flash, 1987). This research methodology represents a powerful tool for neuroscience investigation. However, it is still affected by an important drawback: the “reality gap”. Indeed, mathematical models of complex physical phenomena, such as the interaction between the human arm and the external environment, always present a discrepancy with the real world. This could results in a divergence between the simulation result and real-world behavior, possibly reducing the usefulness of the model.

As a complement to mathematical analyses, the implementation of a given neuroscientific hypothesis on a real mechanical system can reveal the effects of unmodelled dynamics, overcoming the reality gap problem. This is the reason why it is necessary to have a robotic model of the human arm that replicates the key mechanical behaviour of the human neuromuscular system. As such, an accurate robotic model of the human arm could provide a tool under the full control of the experimenter, reproducing the main functional features of the human arm and being able to interact with the same physical environment of the human.

Based on the above analysis, over the past six years we developed the anthropomorphic 2-DOF planar robotic arm NEURARM, a robotic model of the human arm under the full control of the experimenter (Vitiello et al., 2007; Vitiello et al., 2008; Cattin et al., 2008; Vitiello et al., 2010; Lenzi et al., 2011).

Requirements for the design of the NEURARM originated from the investigation of some of the major works on the human motion control theories. In particular, we started from the fact that the motion control strategy used by the CNS to control our own body is still under debate (Hinder and Milner, 2003). Among the main theories, the 'equilibrium point hypothesis' (EPH) (Hogan, 1984; Hogan, 1985; Hogan et al., 1987; Bizzi et al., 1984; Polit and Bizzi, 1979), and the 'interior model hypothesis' (IMH) (Kawato, 1999; Wolpert et al., 1995; Wolpert et al., 1999; Flanagan and Wing, 1995), while being completely different, are of great interest.

According to the EPH, CNS can generate stable angular equilibrium postures, towards which the arm is attracted, by properly regulating the activation levels of antagonistic muscles and with no knowledge of the human arm dynamic behaviour. Conversely, according to IMH, CNS uses the muscle activation to directly control the joint torque taking into account a prior knowledge of the dynamic behaviour of the system.

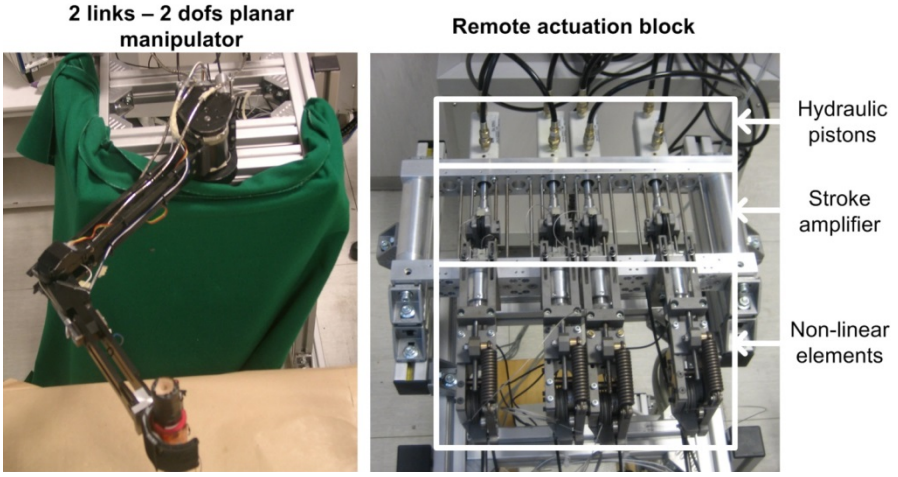

Fig. 8. From Lenzi et al. (Biological Cybernetics 2011). Overview of the NEURARM platform (with kind permission from Springer Science+Business Media).

In order to realize a robotic tool that could be used for addressing investigations with both the above strategies, the NEURARM design addressed two key requirements. First, the robot kinematic parameters and inertia should be similar to that of the human being. Second, the robot actuation should mimic the main physical features of the human actuator system, such as: (i) the use of tendons to transfer force; (ii) passive elasticity of muscles in absence of any neural feedback; (iii) implementation of antagonistic pairs of muscles; (iv) non-linearity of the elastic behaviour allowing modulation of net stiffness through co-activation of opposing muscles.

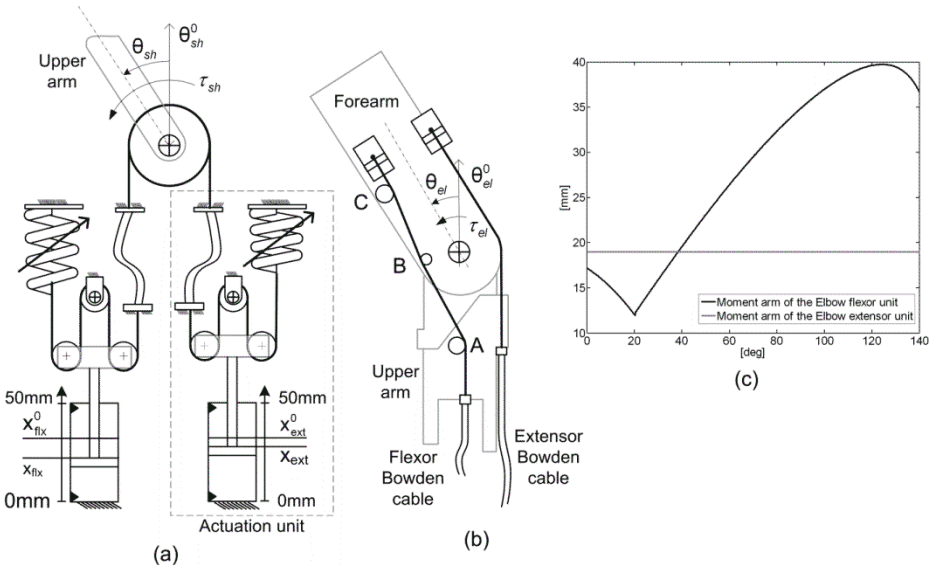

Fig. 9. From Vitiello et al. (Mechatronics 2010). NEURARM joints. (a) Shoulder joint. (b) Elbow joint. (c) Flexor moment art vs. joint angle of the NEURARM elbow joint (reprinted with permission from Elsevier).

5.2 Overview of the Robotic Platform

The NEURARM platform is a 2-link-2-DOF planar robotic arm with two revolute joints, the shoulder and the elbow, whose rotation axes are perpendicular to the motion plane, and two aluminium links, the upper arm and the forearm. The current setup of the NEURARM platform is shown in Fig. 8.

Both the NEURARM shoulder and elbow joints are driven by a pair of antagonist actuation units. However, the two joints have a different configuration. The shoulder, whose motion range is in the interval [-90°, 90°], consists of a pulley with a diameter of 60 mm, on which the antagonist cables reel and can generate a torque by means of a constant moment arm equal to 30 mm (Fig. 9-a). The elbow joint, thoroughly described in (Cattin et al., 2008), has a motion range in the interval [0°, 140°], is more complex and mimics the tendon routing of the human elbow (Kapandji, 1982; Fagg, 2000) (Fig. 9-b). The cables for the extension and flexion of the elbow are directly attached on the forearm. For the extensor rope, the elbow behaves like a pulley with a

constant radius equal to 19.5 mm. The flexor rope, because of its particular path around the rotating shaft A, and the two pins B and C, has a moment arm that is a non-linear function of the joint angle. The analytical model used to get the description of the non-linear function can be found in (Cattin et al., 2008). The function of the flexor moment arm vs. the elbow joint angle is shown in Fig. 9-c. For both the shoulder and elbow joints, the joint is flexing when the joint speed is positive, and it is extending when it is negative.

The NEURARM joint actuation system replicates the human musculoskeletal system configuration by means of two antagonist compliant actuators (Vitiello et al., 2010; Lenzi et al., 2011). As illustrated in Fig. 9-a, each antagonist actuation unit consists of three functional elements:

- a non-linear elastic element emulating the muscle's passive elastic behaviour;
- a linear hydraulic actuator combined with a stroke amplifier to mimic the contractile capability of the muscle. These two elements allow the regulation of the rest length of the non-linear elastic element. The hydraulic piston is the active component of the transmission system, while the stroke amplifier is used to transform a piston displacement into a four-time higher cable displacement This latter element satisfies the system requirement in terms of contraction velocity and force generation, and allows one to achieve performance similar to that of the human arm;
- a steel cable transmitting the force to the NEURARM joint by means of a Bowden cable.

Both the non-linear springs and the hydraulic actuators are located remotely from the robot. This solution satisfies the requirements for the mass and inertia of the links without affecting the system's capability to functionally emulate the human musculoskeletal system. This would not have been possible with an on-board actuation solution. Moreover, thanks to the low weight and high flexibility of the Bowden cables, the power is transferred to the joints without affecting the arm kinetics and kinematics.

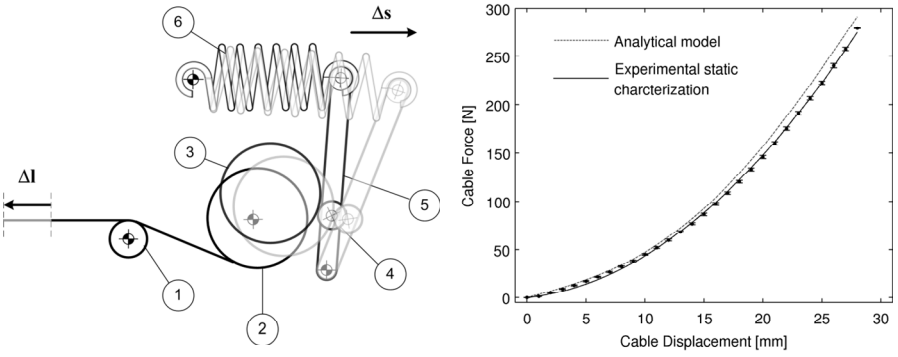

(a) (b)

Fig. 10. From Lenzi et al. (Biological Cybernetics 2011). (a) Schematic representation of the non-linear spring. (1) Idle pulley. (2) Reel. (3) Cam. (4) Idle wheel. (5) Bar. (6) Tension spring. (b) Comparison between numerical model and experimental data of the non-linear spring (with kind permission from Springer Science+Business Media).

5.3 The Non-Linear Elastic Element

The design of the non-linear elastic element was of crucial importance to mimic the human muscle characteristics. Its main design requirements were:

- the force (F) vs. elongation (Δl) characteristic should be well approximated by a quadratic polynomial curve $F(\Delta l) = a_1 \Delta l^2 + a_2 \Delta l$; such that the force increases with elongation and the stiffness ($dF/\Delta l$) increases with force;
- the linear stiffness of the spring, coupled with the tendon transmission around the joints should result in a joint stiffness range for the shoulder and the elbow joint of about 40 $N \cdot m \cdot rad^{-1}$, based on measured values of human arm stiffness in static position (Mussa-Ivaldi et al., 1985) or during movement (Gomi and Kawato, 1997; Burdet et al., 2000).

Starting from a linear tension spring, we designed a low-friction mechanism to obtain the non-linear elastic behavior. The mechanism works in a two-stage fashion. First, it establishes a non-linear relationship between the displacement of the cable (Δl), and the elongation of the linear tension spring (Δs). Second, the force exerted by the linear-tension spring $F_{\Delta s}$ is transformed into a force on the cable $F_{\Delta l}$ by a cam mechanism.

As illustrated in the schematic representation of Fig. 10-a, the mechanism consists of six elements and the working principle can be summarized in five steps: (i) the steel cable is deflected by an idle pulley (*body* 1) and then wrapped around a reel (*body* 2) which is fixed with a cam (*body* 3); (ii) the cam transmits the force and the movement to a bar (*body* 5) by means of an idle wheel (*body* 4), minimizing the friction; (iii) the bar is hinged down on the frame and is connected at its opposite extremity to the tension spring (*body* 6), which is hinged on the frame; (iv) a displacement Δl of the cable rotates the reel and consequently the cam; (v) the cam moves the bar via the idle wheel, and so the tension spring is stretched of Δs.

A detailed modelling of the non-linear elastic mechanism was presented in (Lenzi et al., 2011), while a detailed experimental characterization was given in (Vitiello et al., 2008). A comparison between the numerical model and the results from the experimental characterization are recapped in Fig. 10-b. Results pointed out that the non-linear force/elongation curve was well approximated by a second order polynomial function.

5.4 Control Strategies of the NEURARM

In order to use the NEURARM as a robotic model to explore both EPH- and IMH-based control hypotheses, we implemented two control strategies:

- an *independent control of the NEURAMR joint position and stiffness*, derived from the investigations on the EPH;
- a *sensorless joint torque control*, in this case the NEURARM joints were modelled as Antagonistic Driven Compliant Joints (ADCJ), a particular case of compliant joint.

Both the above control strategies relied on a lower-level closed-loop position controller of the four hydraulic pistons, each controlled by means of a three-land-four-way proportional electronic valve: the control signal being the reference of the spool

valve position, and actually fixing the piston velocity, as explained in (Vitiello et al., 2007; Vitiello et al., 2008). The hydraulic circuit was powered by a three-phase 1.1 kW AC motor (Parker-Hannifin Corp., OH, USA).

The control system runs on a real-time controller, a NI-PCI-8196 RT (National Instruments, Austin, Texas, US), endowed with three data acquisition cards M-series (National Instruments, Austin, Texas, US). Two digital incremental encoders (resolution of 0.05°) are used to measure the joints position and four linear potentiometers (resolution of 0.01 mm) for the measurement of the pistons position. Finally, the NEURARM end-effector can be equipped with a 6-axis load cell in order to measure the interaction force between the robotic arm and the environment.

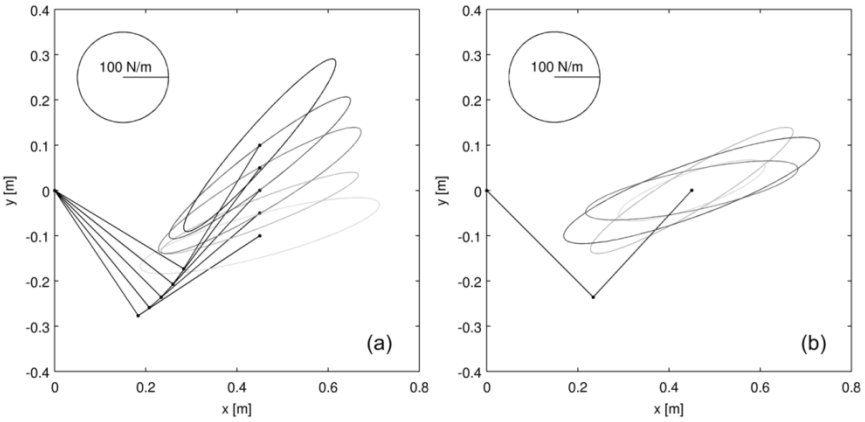

Fig. 11. From Lenzi et al. (Biological Cybernetics 2011). Estimates stiffness ellipses for: (a) different positions and fixed joint stiffness and, (b) different joint stiffness and fixed position (with kind permission from Springer Science+Business Media).

Independent Joint Position and Stiffness Control

The independent control of the joint position and stiffness relies on the following biomimetic concept. When two non-linear elastic springs are coupled to act around a single joint, the opposing torques generated by each elastic element will result in a convergent torque field around a virtual equilibrium position θ_{eq} (i.e. the static position that the arm would reach if no external loads are applied). The equilibrium point as well as the torque field slope (i.e. joint stiffness) will be directly determined by the positions of the two hydraulic pistons. By properly moving the pistons the joint equilibrium point and stiffness change. To show how it is possible to independently adjust the equilibrium position and the joint stiffness, a mathematical description of the actuation scheme working principle is given in (Lenzi et al., 2011). For instance, for the NEURARM shoulder the following equations for equilibrium position θ_{eq}^{sh} and stiffness K_{θ}^{sh} apply:

$$\theta_{eq}^{sh} = a_f\left(x_{ext}^{sh} - x_{flx}^{sh}\right)/2R \tag{1}$$

$$K_{\theta}^{sh} = -2R^2(a_2 - a_1 a_f(x_{ext}^{sh} + x_{flx}^{sh})) \tag{2}$$

where a_f is the stroke amplifier transmission ratio, x_{ext}^{sh} and x_{flx}^{sh} are the shoulder flexor and extensor piston positions, R is the shoulder pulley radius. From the above equations it is evident that the shoulder joint equilibrium position is proportional to the difference between the two piston positions, while the joint stiffness depends on their sum. Thereby, the joint position and stiffness can be regulated independently. Similar – but more complex, given the non-linear function between the flexor moment arm and the joint angle - equations can be written for the elbow joint, as it is well described in (Lenzi et al., 2011).

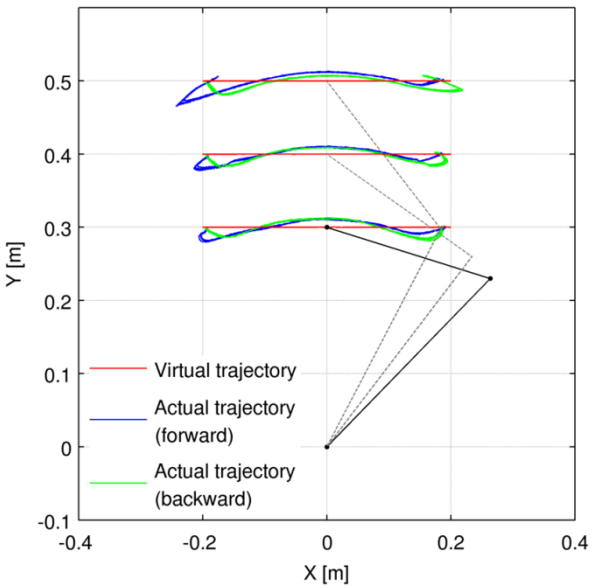

Fig. 12. From Lenzi et al. (Biological Cybernetics 2011). Cartesian space reaching tasks: three different end point virtual paths are tested by performing 10 iteration, back and forth for each trajectory (with kind permission from Springer Science+Business Media).

In the work (Lenzi et al., 2011) we also evaluated the performance of the independent joint position and stiffness control. In particular, performance can be summarized in the following main points.

- The static torque-angle characterization showed that the joint stiffness could be actively tuned in the range 6.5-21 N·m·rad^{-1} for the shoulder and 1.7-8.5 N·m·rad^{-1} for the elbow (Lenzi et al., 2011).
- The step response of the joints position controller - recorded for different stiffness levels – pointed out that the natural frequency of the shoulder joints increases from 1.1 Hz to 1.53 Hz (damping ratio increasing from 0.138 to 0.173) at the increase of the joint stiffness when the elbow joint is fully extended, and from 1.49 Hz to 2.13 (damping ratio increasing from 0.142 to 0.192) when the elbow joint is fully flexed.
- The experimental characterization of the end-point stiffness – that was addressed by applying a procedure similar to that used in the characterization of the human

arm spring-like behaviour (Mussa-Ivaldi et al., 1985) – showed that NEURARM could change in a bio-mimetic fashion the end-point stiffness ellipsoid (Fig. 11).
- NEURARM was capable to execute 40-cm rectilinear paths in the Cartesian space by sliding the equilibrium point along a virtual trajectory (i.e. the desired end-effector equilibrium position) with a bell shaped velocity profile, with a duration of 1 s (Fig. 12) with performance comparable to the numerical simulation performed in (Hogan 1984, Flash 1987) and consistent with direct observations on the human being (Gomi and Kawato, 1997).

Sensorless Torque Control

From an engineering view point, the research activities carried out for the development of a sensorless torque control are framed within the research field of robotic compliant joints. Compliant joints are receiving increasing attention in current robotics research, representing one of the best solutions to actuate robots involved in *cooperative tasks with humans*. It is current opinion that conventional robot technology, in which the robot actuators are designed primarily as rigid positioning devices or torque sources, is not able to match safety requirements in human-robot interaction. For instance, in collaborative tasks, a rigid robot could present great risks in case of a collision, as common software interaction controls require some time to react and adjust the compliance of the robot after the detection of the impact. On the other hand, the mechanical properties of hardware compliant robots, together with an appropriate control scheme, can make the robot safer (Van Damme et al., 2009). Moreover, compliant joints improve the robotic system robustness by making the overall system more tolerant to unpredictable changes in the models of the environment and of the robot, as well as in the dynamics of the human they are interacting with (Pfeifer et al., 2005; Filippini et al., 2008; Vanderborght et al., 2009).

These properties make the use of compliant joints appropriate for application in robots for personal assistance and rehabilitation (Vallery et al., 2008). Pratt and Williamson (1995) proposed one of the first examples of compliant joints, the Series Elastic Actuator (SEA). Following these studies, different examples have been conceived and tested exploiting various working principles and architectures (Collins and Ruina, 2005; Hurst and Rizzi, 2008; Mao et al., 2007; Van Ham et al., 2007).

The NEURARM joints can be classified as Antagonistic Driven Compliant Joint (ADCJ), one of the most studied configurations in the last years. This solution has two peculiar characteristics: (i) the joint is powered by two independent actuation units; (ii) each actuation unit works functionally as a non-linear elastic element with an adjustable resting position.

Several different engineering solutions based on the ADCJ configuration have been investigated. Schiavi et al. (2008) designed the variable stiffness actuator VSAII, using a 4-bar mechanism along with a linear spring as a non-linear element. Migliore et al. (2005) presented a tendon-driven ADCJ, in which the non-linear element consisted of a spring wrapped in a kinematic mechanism. Koganezawa et al. (2006) presented the Actuator with Non Linear Elastic System (ANLES), consisting of a DC motor rotating a guide shaft connected to the transmission board via a torsion spring. In this kind of actuators, the joint was controlled by means of two independent position-stiffness regulators. Pneumatic muscle actuators (pMA) were also exploited for developing ADCJ (Caldwell et al., 1995; Jutras and Bigras, 2006; Lilly, 2003; Tsagarakis and Caldwell, 2003; Tondu et al., 2005).

Majority of the algorithms exploited to control ADCJs are aimed at regulating the joint position and stiffness independently, as in the case of the *biological inspired joint stiffness control* presented by Migliore, or the independent joint position and stiffness control of the NEURARM. Nevertheless, there are some cases in which a direct control of the joint torque is required. For instance, for application in rehabilitation and assistive robotics, the robotic device (e.g. exoskeleton, Cartesian manipolandum) is often required to support the disabled person by providing a controllable force/torque (Vallery et al., 2008).

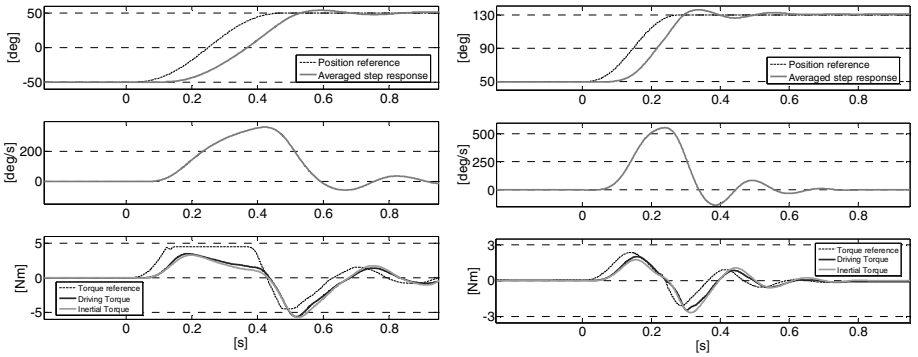

Fig. 13. From Vitiello et al. (Mechatronics 2010). Execution of the single-joint trajectories: (a) Shoulder joint. (b) Elbow joint. Top panel: desired and actual position. Middle panel: actual joint velocity. Bottom panel: desired driving torque, actual driving torque and inertial torque. Actual trajectories are averaged over 20 iterations (reprinted with permission from Elsevier).

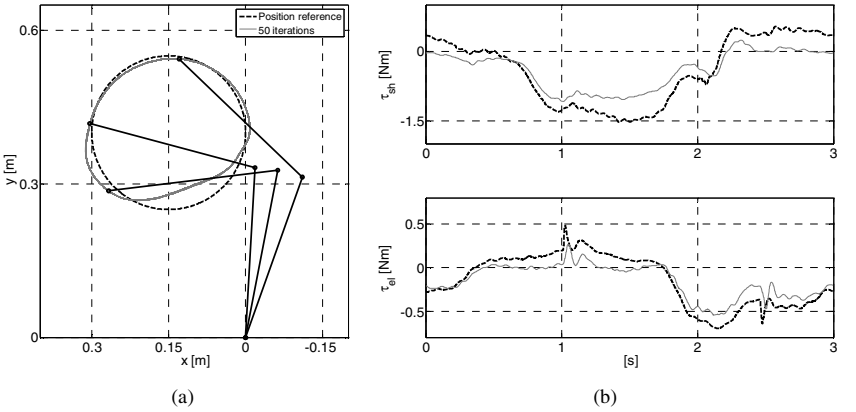

Fig. 14. From Vitiello et al. (Mechatronics 2010). Cartesian space multi-dof trajectories. (a) Desired and actual Cartesian trajectory. (b) Desired and actual driving torque. Top panel: shoulder torque. Bottom panel: elbow torque. Actual trajectories are averaged over 50 iterations (reprinted with permission from Elsevier).

Within this framework we developed a "sensorless" torque control strategy suitable for ADCJs based architectures. The proposed strategy does not require any additional force/torque sensors, and can be applied to all the ADCJs usually controlled through a position/stiffness regulator. The proposed sensorless torque control strategy can be explained as follows (Vitiello et al., 2010).

- An ADCJ is powered by a couple of independent actuation units, named flexor and extensor units. Each unit implements a non-linear spring whose resting position is controlled by a dedicated motor. The resulting torque τ acting on the joint depends on the forces applied respectively by the flexor F_{flx} and extensor F_{ext} actuation units, and, possibly, on the joint angular position θ: $\tau = h(F_{flx}, F_{ext}, \theta)$. For instance, in the case of an ADCJ consisting of a pulley-driven joint, the torque is simply dependent on the actuation units force difference, while in the case of a lever-driven joint, the force arms not being constant, the torque is also function of the joint angle (Vanderborght et al., 2009). Therefore, a suitable strategy to control the joint torque is to properly and independently control the force powered by each actuation unit.
- In order to control the actuation unit force, and consequently the joint torque, without using any force/torque sensor, a strategy to estimate these forces is needed. The proposed method relies on the actuation unit elastic property: because of this, each unit exerts a force F function of its elongation Δl: $F = f_{NL}(\Delta l)$, where f_{NL} is a generic non-linear function, and Δl depends on the joint angular position and the motor position x through a function g: $\Delta l = g(\theta, x)$.
- Since θ and x can be measured, the force F can be estimated if the functions f_{NL} and g are known. In particular, the function g can be obtained from kinematic considerations while f_{NL} from an experimental characterization. The experimental characterization is a key point of the proposed strategy because it is a reliable way to model in f_{NL} the effects of: (i) the undesired elastic action of flexible transmission means, such as tendon wires or belts; (ii) Coulomb friction introduced by high-friction transmission elements, such as Bowden cables.
- Assuming that the functions h, g and f_{NL} are known, it is then possible to exploit the indirect estimation of F to perform a closed-loop control of the force powered by each actuation unit, and consequently the resulting torque τ on the joint.

In the work (Vitiello et al., 2010) we actually employed the above strategy to develop a joint torque control for NEURARM. Performance of the proposed torque control strategy are summarized in the following main points.

- The torque control bandwidth was higher than 10 Hz for both shoulder and elbow joints; in the step response the control accuracy at the steady state was in the range 0.02-0.04 N·m.
- The developed torque control strategy was successfully benchmarked against the execution of both single- (Fig. 13) and multi-joint trajectories (Fig. 14), with a bell-shaped velocity profile with a peak of 300 deg·s^{-1} and 500 deg·s^{-1}, respectively for the shoulder and the elbow joints.

5.5 Remarks

The experimental activities carried out with the NEURARM had an immediate and strong impact on the design and development of the elbow exoskeleton NEUROExos, which is described in the following section. Indeed, for the actuation of the first prototype of NEUROExos we employed the same biomimetic antagonistic actuation we developed for the NEURARM. Thanks to this choice we could endow NEUROExos with an adaptive joint impedance, which is typical of the human arm. Furthermore, because of its variable impedance antagonistic actuation, NEUROExos can interact with human subjects with the appropriate joint output impedance. For instance NEUROExos can be "stiff" (and modulate its stiffness) when it is requested to drive the human motion or "transparent" when it has to constructively cooperate with humans. In other terms, thanks to its adjustable joint compliance NEUROExos can address the execution of both *robot-in-charge* and *patient-in-charge* rehabilitation exercises.

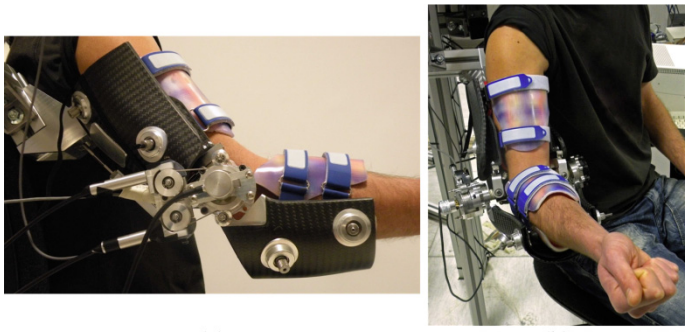

Fig. 15. Overview of the NEUROExos. (a) Lateral view. (b) Front view. © 2013 IEEE. Reprinted, with permission, from Vitiello et al. (IEEE Transactions on Robotics 2013).

6 NEUROExos: An Elbow Robotic Exoskeleton

6.1 Background

Robot-aided physical rehabilitation has been proposed to support physicians in providing high-intensity therapy, consisting of repetitive movements of post-stroke impaired limbs (Barreca et al., 2003; Feys et al., 1999; Kwakkel et al, 1999). The use of robots enable the patients to receive the benefits from the rehabilitation process, while the therapists can reduce their workload. Moreover, the robotic device offers an objective, reliable means of monitoring the patient progress.

State-of-the-art devices for upper limb robot-assisted therapy can be classified in: end-point manipulators (Krebs et al., 1998; Fasoli et al., 2003; Lum et al., 1999; Micera et al., 2006; Reinkensmeyer et al., 2001), cable suspensions (Mayhew et al., 2005; Stienen et al., 2007), and exoskeletons (Jia-Fan et al., 2008; Kiguchi et al., 2004; Perry et al., 2007; Frisoli et al., 2007; Frisoli et al., 2009; Tsagarakis and Caldwell, 2003; Carignan et al., 2007; Rocon et al., 2007; Nef et al., 2007; Mihelj et al.,

2007; Sanchez et al., 2006; Sanchez et al., 2007; Schiele and van der Helm, 2006; Stienen et al., 2009). Among these, the latter was proposed as a solution to the problem of control and measurement of angle and torque on each joint of the impaired limb (Stienen et al., 2009).

An exoskeleton for post-stroke physical rehabilitation is a nonportable mechanical device that is anthropomorphic in nature, is "worn" by the user, and fits closely to his or her body (Dollar and Herr, 2008). Given the close interaction with the user, comfort is a major concern. An exoskeletal robot for physical rehabilitation should be lightweight and take into account the user's joints range of motion (ROM), anthropometry, and kinematics (Schiele and van der Helm, 2006; Stienen et al., 2009). The physical human–robot interaction (pHRI) area should be large and should match the shape of the patient's limb to reduce the pressure on the user's skin (Rocon et al., 2007; Pons, 2010). Furthermore, the actuation and control of the robot should allow safe execution of rehabilitation exercises in two modes of operation: *robot-in-charge*, when the robot is driving the subject in doing the exercises, and *patient-in-charge*, when the subject is driving the robot that is only partially assisting the movement (Krebs et al., 1998).

The NEUROROBOTICS Elbow Exoskeleton (NEUROExos) was introduced in the state of the art with three innovative design solutions (Fig. 15): (i) a compact and light-weight mechanical structure with double-shelled links, with a wide pHRI area to minimize the pressure on the skin; (ii) a 4-DOF passive mechanism that unloads the elbow articulation from undesired loads by ensuring the alignment of human and robot joint axes; (iii) the biomimetic, remote antagonistic actuation unit developed for the robotic arm NEURARM (Lenzi et al., 2011; Vitiello et al., 2013).

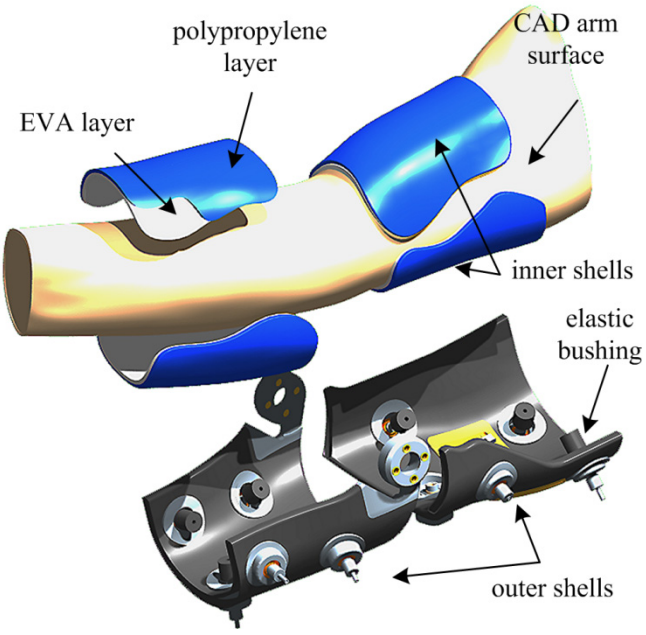

Fig. 16. Double-shelled structured links. © 2013 IEEE. Reprinted, with permission, from Vitiello et al. (IEEE Transactions on Robotics 2013).

6.2 System overview

The NEUROExos is a mechatronic device, constituted of the following four subsystems: (i) two double-shell structured links, (ii) a 4-DOF passive mechanism, (iii) a remote, antagonistic tendon-driven compliant actuation, (iv) a control system and a sensory apparatus.

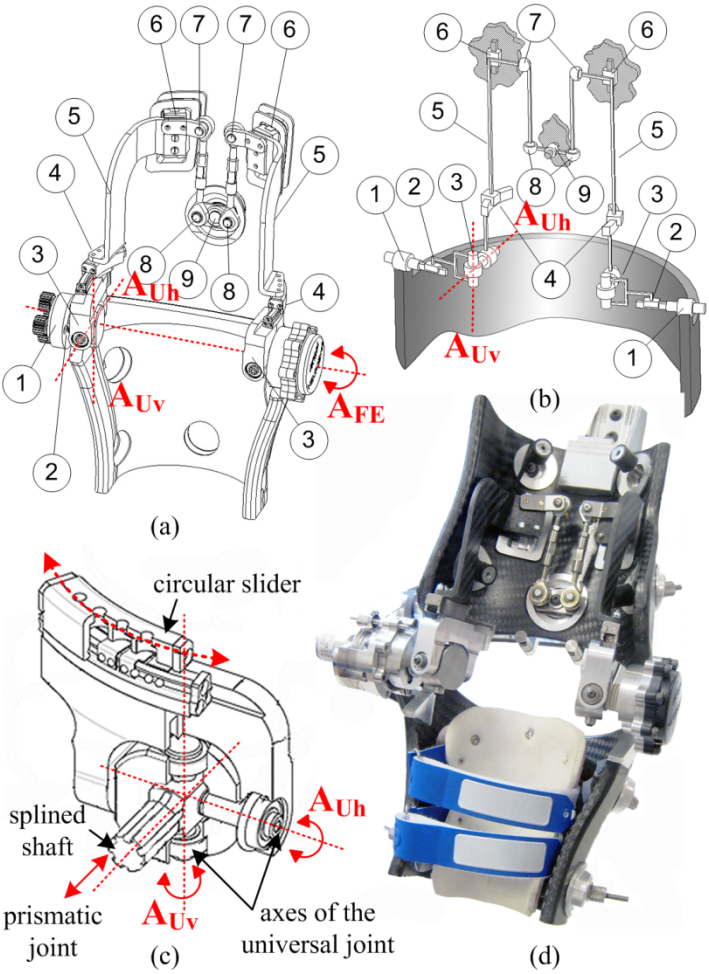

Fig. 17. 4-DOF passive mechanism. (a) CAD and (b) layout of the passive mechanism. (1) NEUROExos flexion–extension joint, axis A_{FE}. (2) Prismatic joint through splined shaft. (3) Universal joint. (4) Circular slider. (5) Carbon fiber link. (6) Linear slider. (7) Spherical joint. (8) Spherical joint. (9) Rotational joint. (c) Zoom on joints (1), (2), (3), and (4). A_{Uv} and A_{Uh} are the vertical and horizontal rotational axes of the universal joint; the splined shaft allows for the prismatic joint (2) whose axis coincides with A_{FE} (d) Implementation of the passive mechanism. © 2013 IEEE. Reprinted, with permission, from Vitiello et al. (IEEE Transactions on Robotics 2013).

Double-Shelled Links

The NEUROExos links were conceived in a way that the interaction force between the user and the robot should be distributed over a wide area, which should fit the shape of the human limb segments. Linkages were developed by taking into account the inter-subject variability and have low weight, inertia, and encumbrance, while ensure a good level of flexional stiffness to sustain the interaction torque.

The solution implemented for NEUROExos is depicted in Fig. 16. Each link is composed of two concentric shell-like structures.

Inner shells come in different sizes, and can be tailor-made on each subject (e.g., by thermo shaping a polypropylene layer). Each inner shell is made of two half-shells, to be coupled with the dorsal and ventral sides of the limb segment. Inner shells have a structure composed by two layers: a 3 mm-thick internal layer of ethylene vinyl acetate (555XEB/3, M.T.O., Italy), which is in contact with the skin of the patient and has properties of moisture draining and skin transpiration, and a 3 mm-thick outer layer of polypropilene (558/3, M.T.O., Italy).

Outer shells have a double-walled carbon fiber structure, which has a total height of 10 mm and thickness of 1.5 mm. Outer shells can be connected to inner shells of different shapes, and, therefore, enable the same exoskeleton links to be used by several users. Outer shells also house the aluminium frames of the 4-DOF passive mechanism, the gear box for the active flexion–extension DOF, and the inner–outer shell connecting elements. Connecting elements consist of an aluminium frame housed inside the carbon fiber structure and containing a passive spherical joint (GE 8C, SKF, Sweden) and an elastic bushing (Radialflex M4, Paulstra, France). Spherical joint and elastic bushing allow small relative motions between inner and outer shells and thus enhance comfort.

4-DOF Passive Mechanism

In order to guarantee the best kinematics matching between human and robot rotation axes, NEUROExos was equipped with a 4-DOF passive mechanism (Fig. 17). This mechanism is implemented by means of a closed-chain mechanism composed of 13 passive joints: 4 prismatic, 4 spherical, 2 circular sliders, 2 universal and 1 rotational joints. The flexion-extension axis A_{FE} is identified by means of the two axes of the prismatic joints (labeled as 2 in Fig. 17). These joints are implemented by means of two splined shaft-hole couplings having a range of motion (ROM) of 35 mm. Each splined shaft is attached to a universal joint (labeled as 3 in Fig. 17), whose ROM is 100° around the axis A_{Uh} and 24° around the axis A_{Uv}. Each fork housing one universal joint is then attached to a slider (joint number 4 in Fig. 17) moving along a circular trajectory having a diameter of 250 mm and an angular ROM of 42°. Through a carbon fiber link, the circular slider is connected to a linear slider (joint number 6 in Fig. 17, ROM of 30 mm). The linear slider is linked to the rotational joint labeled as 9 in Fig. 17 (ROM of 40°) by means of two spherical joints (male threaded, maintenance-free rod ends, SKF, Göteborg, Sweden) labeled as 7 and 8, connected by a bar with an adjustable length.

The passive mechanism provides A_{FE} with three passive DOFs, which allow the NEUROExos axis to trace the same double conic frustum traced by the human axis

(Bottlang et al., 1998; Bottlang et al., 2000; Duck et al., 2003). First, A_{FE} can rotate in the frontal plane of an angle $\gamma_f = \pm 15°$. Then, A_{FE} can rotate in the horizontal plane of an angle $\gamma_h = \pm 21°$. Finally, the NEUROExos forearm link can slide along the axis A_{FE}.

Finally, A_{FE} can translate onto the horizontal plane along the antero-posterior direction of a segment $\Delta = \pm 15$ mm. This translational DOF is fundamental to partly compensate for the undesired forces which are caused by the joint axes misalignment (Stienen et al., 2009).

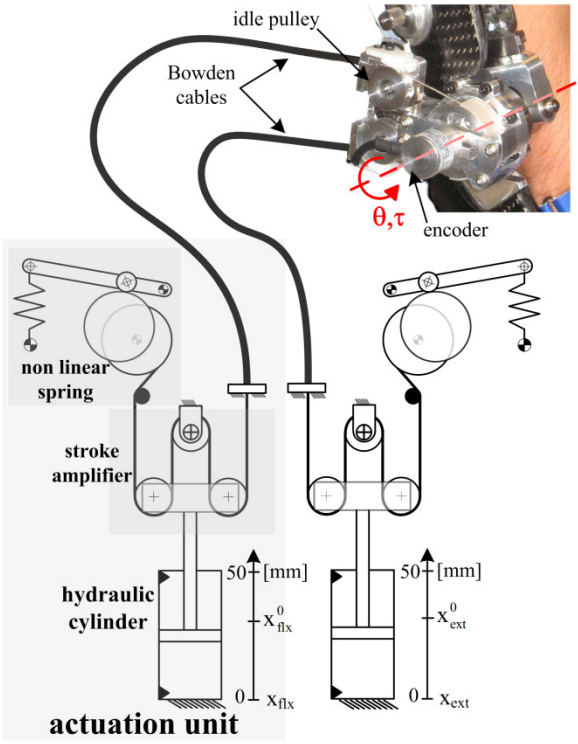

Fig. 18. Schematic drawing of the antagonistic tendon-driven compliant actuation and sensory system of the NEUROExos. Two remote antagonistic units, which are named flexor ("flx") and extensor ("ext"), power the NEUROExos active joint. © 2013 IEEE. Reprinted, with permission, from Vitiello et al. (IEEE Transactions on Robotics 2013).

Antagonistic Compliant Actuation

The layout of the actuation system of NEUROExos is depicted in Fig. 18. It consists of a pair of remote and independent antagonistic units, which are similar to those used for the actuation system of the anthropomorphic robotic arm NEURARM: in this case we used a tension spring of 80 $N \cdot mm^{-1}$ so that NEUROExos can achieve an actively adjustable passive joint stiffness in the range 20-60 $N \cdot m \cdot rad^{-1}$. This range is indeed comparable with the one of the human elbow.

Control and Sensory System

The actuation system of NEUROExos allows for the use of two alternative control strategies: the *passive-compliance control* and the *torque control*, respectively for the execution of robot-in-charge and patient-in-charge exercises.

The passive compliance control – as for the NEURARM – allows for an independent joint position and stiffness control by respectively setting the difference and the sum of the piston positions.

The torque control relies instead of the independent closed-loop control of the cable force powered by the each actuation unit. The desired torque τ_{des} is converted into two desired forces on the antagonistic cables. Then, the desired cable forces serve as input of two independent closed-loop force controllers.

Both the NEUROExos control algorithms run on a real-time control system (NI PXI-8196 RT, Austin, TX, USA) equipped with a data acquisition card (NI M-series, Austin, TX, USA). Cable force and pistons positions signals are sampled at 250 kHz, then low-pass filtered and down-sampled to 1 kHz.

NEUROExos is endowed with a 1024 ppr incremental optical encoder (2420, Kübler, Germany) assembled coaxially with the driving pulley (resolution of 0.022°). Two custom-made load cells were included in the design, to measure the force transmitted by the antagonist tendon cables (Accuracy 0.05 N). Two linear potentiometers (SLS095, Penny&Giles, Dorset, UK) are used for the measurement of the pistons positions with an accuracy of 0.01 mm.

6.3 System Performance and Perspectives

In the past years, in addition to the experimental characterization addressed within the work (Vitiello et al., 2013), NEUROExos was also employed in experimental trials that aimed at either exploring new human-machine interfaces (Ronsse et al., 2010; Ronsse et al., 2011; Lenzi et al., 2011b; Lenzi et al., 2012) or testing a novel wearable pressure-sensitive sensor to sense the physical human-robot distributed interaction (Lenzi et al., 2011c; De Rossi et al., 2010; De Rossi et al., 2011; Donati et al., 2013). From this extensive experimentation of the NEUROExos the following main results derived.

- Measurements on five healthy subjects proved that – thanks to the 4-DOF passive mechanism – the NEUROExos rotation axis actually moves along with the elbow flexion-extension, and thus it ensures a safe and comfortable human-robot interaction. Thanks to this result we were motivated to develop a theoretical framework for the design of passive mechanisms for human-robot joint axes self-alignment (Cempini et al., 2013), and to apply the same idea on a hand exoskeleton (Chiri et al., 2012; Cempini et al., 2013b).
- Under the passive-compliance control, the NEUROExos passive stiffness can be actively tuned in the range The torque control bandwidth was higher than 10 Hz for both shoulder and elbow joints; in the step response the control accuracy at the steady state was in the range 24-56 $N \cdot m \cdot rad^{-1}$; the equilibrium point can be changed with a -3-dB bandwidth of about 7 Hz.

- Under the action of the torque control, the NEUROExos joint is highly transparent: its output impedance increases across the spectrum, and it changes from 1 $N \cdot m \cdot rad^{-1}$, for 0.3 Hz motion, up to 1 $N \cdot m \cdot rad^{-1}$, for 3.2 Hz motion. The closed-loop torque control bandwidth is higher than 10 Hz.

Recently a new version of the NEUROExos was developed, which is endowed with a new actuation unit based on a compact, light-weight series-elastic actuator. This new version was early presented in a conference paper and is currently employed in an extensive clinical trial in the rehabilitation center "Auxilium Vitae", in Volterra, Italy.

References

André, T., Lefèvre, P., Thonnard, J.-L.: A continuous measure of fingertip friction during precision grip. Journal of Neuroscience Methods (2009)

Astarloa, A., Lazaro, J., Bidarte, U., Jimenez, J., Zuloaga, A.: FPGA technology for multiaxis control systems. Mechatronics 19(2), 258–268 (2009)

Barreca, S., Wolf, S.L., Fasoli, S., Bohannon, R.: Treatment interventions for the paretic upper limb of stroke survivors: a critical review. Neurorehabilitation and Neural Repair 17(4), 220–226 (2003)

Beckmann, S., Bjrnsdotter, M., Backlund-Wasling, H., Wessberg, J.: Brain decoding of texture processing using independent component analysis and support vector machines. In: Proc. 2009 IEEE International Symposium on Intelligent Signal Processing, Budapest, Hungary, pp. 287–292 (2009)

Bekey, G.: Autonomous Robots. From Biological Inspiration to Implementation and Control. The MIT Press, US (2005)

Birznieks, I., Jenmalm, P., Goodwin, A.W., Johansson, R.S.: Encoding of direction of fingertip forces by human tactile afferents. J. Neurosci. 21, 8222–8237 (2001)

Bizzi, E., Accornero, N., Chapple, W., Hogan, N.: Posture control and trajectory formation during arm movement. Journal of Neuroscience 4, 2738–2744 (1984)

Bliss, J.C., Katcher, H., Rogers, C.H., Shepard, R.P.: Optical-to-Tactile Image Conversion for the Blind. IEEE Transactions on Man-Machine Systems 11, 58–65 (1970)

Bonsignori, G., Stefanini, C., Scarfogliero, U., Mintchev, S., Benelli, G., Dario, P.: The green leafhopper, Cicadella viridis (Hemiptera, Auchenorrhyncha, Cicadellidae), jumps with near-constant acceleration. The Journal of Experimental Biology 216(7), 1270–1279 (2013)

Bottlang, M., Madey, S.M., Steyers, C.M., Marsh, J.L., Brown, T.D.: Factors influencing accuracy of screw displacement axis detection with a DC-based electromagnetic tracking system. Journal of Biomechanical Engineering 120(3), 431–435 (1998)

Bottlang, M., Madey, S.M., Steyers, C.M., Marsh, J.L., Brown, T.D.: Assessment of elbow joint kinematics in passive motion by electromagnetic motion tracking. Journal of Orthopaedic Research 18, 195–201 (2000)

Burdet, E., Osu, R., Franklin, D.W., Milner, T.E., Kawato, M.: The central nervous system stabilizes unstable dynamics by learning optimal impedance. Nature 414, 446–449 (2001)

Burdet, E., Osu, R., Franklin, D.W., Milner, T.E., Yoshioka, T., Milner, T., Kawato, M.: A method for measuring end-point stiffness during multi-joint arm movement. Journal of Biomechanics 33(12), 1705–1709 (2000)

Byrne, J.: A feedback controlled stimulator that delivers controlled displacements or forces to cutaneous mechanoreceptors. IEEE Trans. Biomed. Eng. 22, 66–69 (1975)

Caldwell, D.G., Medrano-Cerda, G.A.: Goodwin M, Control of pneumatic muscle actuators. IEEE Contr. Sys. Mag. 15(1), 40–48 (1995)

Carignan, C., Tang, J., Roderick, S., Naylor, M.: A Configuration-Space Approach to Controlling a Rehabilitation Arm Exoskeleton. In: Proc. IEEE International Conference on Rehabilitation Robotics (ICORR), Noordwijk, The Netherlands, pp. 524–531 (2007)

Carrozza, M.C., Cappiello, G., Micera, S., Edin, B.B., Beccai, L., Cipriani, C.: Design of a cybernetic hand for perception and action. Biological Cybernetics 95(6), 629–644 (2006)

Cattin, E., Roccella, S., Vitiello, N., Clemens, E., Sardellitti, I., Panagiotis, K.A., Vacalebri, P., Vecchi, F., Carrozza, M.C., Kyriakopulos, K., Dario, P.: Design and Development of a Novel Robotic Platform for Neuro-Robotics Applications: the NEURobotics ARM (NEURARM). Advanced Robotics, Special Issue on Robotics Platforms for Neuroscience 22, 3–37 (2008)

Cempini, M., De Rossi, S.M.M., Lenzi, T., Cortese, M., Giovacchini, F., Vitiello, N., Carrozza, M.C.: Kinematics and Design of a Portable and Wearable Exoskeleton for Hand Rehabilitation. In: Proceedings of the IEEE International Conference on Rehabilitation Robotics, ICORR (2013)

Cempini, M., De Rossi, S.M.M., Lenzi, T., Vitiello, N., Carrozza, M.C.: Self-Alignment Mechanisms for Assistive Wearable Robots: a KinetoStatic Compatibility Method. IEEE Transactions on Robotics 29(1), 236–250 (2013)

Chiri, A., Vitiello, N., Giovacchini, F., Roccella, S., Vecchi, F., Carrozza, M.C.: Mechatronic design and characterization of the index finger module of a hand exoskeleton for post-stroke rehabilitation. IEEE Transactions on Mechatronics 17(5), 884–894 (2012)

Collins, S., Ruina, A.: A bipedal walking robot with efficient and human-like gait. In: Proceedings of the IEEE International Conference on Robotics and Automation, pp. 1983–1988 (2005)

Connor, C.E., Johnson, K.O.: Neural coding of tactile texture: comparison of spatial and temporal mechanisms for roughness perception. J. Neurosci. 12(9), 3414–3426 (1992)

Craelius, W.: The bionic man: restoring mobility. Science 295(5557), 1018–1021 (2002)

Darian-Smith, I., Oke, L.E.: Peripheral neural representation of the spatial frequency of a grating moving across the monkey's finger pad. J. Physiol. 309, 117–133 (1980)

De Rossi, S.M.M., Vitiello, N., Lenzi, T., Ronsse, R., Koopman, B., Persichetti, A., Giovacchini, F., Vecchi, F., Ijspeert, A.J., van der Kooij, H., Carrozza, M.C.: Soft artificial tactile sen-sors for the measurements of human-robot interaction in the rehabilitation of the lower limb. In: Proc. of the 2010 Annual International Conference of the IEEE Engineering in Medicine and Biology Society (EMBC), Buenos Aires, Argentina, pp. 1279–1282 (2010)

De Rossi, S.M.M., Vitiello, N., Lenzi, T., Ronsse, R., Koopman, B., Persichetti, A., Vecchi, F., Ijspeert, A.J., van der Kooij, H., Carrozza, M.C.: Sensing pressure distribution on a Lower-Limb Exoskeleton Physical Human-Machine Interface. Sensors 11, 207–227 (2011)

Dollar, A., Herr, H.: Lower extremity exoskeletons and active orthoses: Challenges and state-of-the-art. IEEE Transactions on Robotics 24(1), 144–158 (2008)

Donati, M., Vitiello, N., De Rossi, S.M.M., Lenzi, T., Crea, S., Persichetti, A., Giovacchini, F., Koopman, B., Podobnik, J., Munih, M., Carrozza, M.C.: A Flexible Sensor Technology for the Distributed Measurement of Interaction Pressure. Sensors 13(1), 1021–1045 (2013)

Edin, B.B., Ascari, L., Beccai, L., Roccella, S., Cabibihan, J.-J., Carrozza, M.C.: Bio-inspired sensorization of a biomechatronic robot hand for the grasp-and-lift task. Brain Research Bulletin 75(6), 785–795 (2008)

Eiber, C.D., Lovell, N.H., Suaning, G.: Attaining higher resolution visual prosthetics: a review of the factors and limitations. Journal of Neural Engineering 10, 11002 (2013)

Ekeberg, Ö., Lansner, A., Grillner, S.: The neural control of fish swimming studied through numerical simulations. Adaptive Behavior 3, 363–384 (1995)

Esquenazi, A., Talaty, M., Packel, A., Saulino, M.: The ReWalk powered exoskeleton to restore ambulatory function to individuals with thoracic-level motor-complete spinal cord injury. American Journal of Physical Medicine and Rehabilitation 91(11), 911–921 (2012)

Fagg, A.H.: A model of muscle geometry for a two degree-of-freedom planar arm, Technical report, University of Massachusetts, [UMI order no: UM-CS- 2003-003] (2000)

Fasoli, S.E., Krebs, H.I., Stein, J., Frontera, W.R., Hogan, N.: Effects of Robotic Therapy on Motor Impairement and Recovery in Chronic Stroke. Archives of Physical Medicine and Rehabilitation 84(4), 477–482 (2003)

Feldman, A.G.: Functional tuning of the nervous system with control of movement or maintenance of steady posture, II: controllable parameters of the muscles. Biophisics 11, 565–578 (1966)

Feldman, A.G.: Once More on the Equilibrium-Point Hypothesis (λ Model) for Motor Control. Journal of Motor Behavior 18(1), 17–54 (1986)

Feys, H.M., De Weerdt, W.J., Selz, B.E., Cox Steck, G.A., Spichiger, R., Vereeck, C.E., Putman, K.D., Van Hoydonock, G.A.: Effect of a therapeutic intervention for the hemiplegic upper limb in the acute phase after stroke. A single-blind, randomized, controlled multicenter trial. Stroke 29(4), 785–792 (1999)

Filippini, R., Sen, S., Bicchi, A.: Toward Soft Robot You Can Depend On. IEEE Robotics and Automation Magazine 15(3), 31–41 (2008)

Flanagan, J.R., Wing, A.M.: The Role of Internal Models in Motions Planning and Control: Evidence from Grip Force Adjustments during Movements of Hand-Held Loads. The Journal of Neuroscience 17(4), 1519–1528 (1995)

Flash, T.: The Control of Hand Equilibrium Trajectories in Multi-Joint Arm Movement. Biological Cybernetics 57, 257–274 (1987)

Frisoli, A., Borelli, L., Montagner, A., Marcheschi, S., Procopio, C., Salsedo, F., Bergamasco, M., Car-boncini, M.C., Tolaini, M., Rossi, B.: Arm rehabilitation with a robotic exoskeleton in Virtual Reality. In: Proc. of IEEE International Conference on Rehabilitation Robotics, Noordwijk, The Netherlands, pp. 631–642 (2007)

Frisoli, A., Salsedo, F., Bergamasco, M., Rossi, B., Carboncini, M.C.: A force-feedback exoskeleton for upper-limb rehabilitation in virtual reality. Applied Bionics and Biomechanics 6(2), 115–126 (2009)

Fukuda, T., Saito, F.: Motion control of a brachiation robot. Robotics and Autonomous Systems 18(1), 83–93 (1996)

Gardner, E.P., Palmer, C.I.: Simulation of motion of the skin. I. Receptive fields and tem-poral frequency coding by cutaneous mechanoreceptors of OPTACON pulses delivered to the hand. J. Neurophysiol. 62, 1410–1436 (1989)

Gomi, H., Kawato, M.: Equilibrium-point control hypothesis examined by measured arm stiffness during multijoint movement. Science 272, 117–120 (1996)

Gomi, H., Kawato, M.: Human arm stiffness and equilibrium-point trajectory during multijoint movement. Biological Cybernetics 76, 163–171 (1997)

Goodwin, A., Morley, J.: Sinusoidal movement of a grating across the monkey's finger-pad: representation of grating and movement features in afferent fiber responses. J. Neurosci. 7, 2168–2180 (1987)

Goodwin, A.W., Morley, J.W., Clarke, C., Lumaksana, B., Darian-Smith, I.: A stimulator for moving textured surfaces sinusoidally across the skin. J. Neurosci. Methods 14, 121–125 (1985)

Grillner, S.: Neurobiological bases of rhythmic motor acts in vertebrates. Science 228(4696), 143–149 (1985)

Grillner, S., Deliagina, T., Ekeberg, O., El Manira, A., Hill, R., Lansner, A., Orlovski, G., Wallen, P.: Neural networks that coordinate locomotion and body orientation in the lamprey. Trends in Neurosciences 18, 270–279 (1995)

Hargrove, L., Simon, A.M., Young, A.J., Lipschutz, R.D., Finucane, S.B., Smith, D.G., Kuiken, T.A.: Robotic Leg Control with EMG Decoding in an Amputee with Nerve Transfers. The New England Journal of Medicine 369, 1237–1242

Hirose, S., Morishima, A.: Design and control of a mobile robot with an articulated body. The International Journal of Robotics Research 9(2), 99–114 (1990)

Hogan, N.: An organizing principle for a class of voluntary movements. Journal of Neuroscience 4, 2745–2754 (1984)

Hogan, N.: Impedance control: an approach to manipulation. Part I: Theory. ASME J. of Dynamic System and Control 107, 1–7 (1985)

Hogan, N.: Impedance control: an approach to manipulation. Part II: Implementation. ASME J. of Dynamic System and Control 107, 8–16 (1985)

Hogan, N.: Impedance control: an approach to manipulation. Part III: Application. ASME J. of Dynamic Systems and Control 107, 17–24 (1985)

Hogan, N., Bizzi, E., Mussa-Ivaldi, F.A., Flash, T.: Controlling multijoint motor behaviour. Exercise and Sport Sciences Reviews 15, 153–190 (1987)

Hurst, J.W., Rizzi, A.A.: Series compliance for an efficient running gait: lessons learned from the electric cable differential leg. IEEE Robot Autom. Mag. 15(3), 42–51 (2008)

Iskakov, R., Albu-Schaeffer, A., Schedl, M., Hirzinger, G., Lopota, V.: Influence of sensor quantization on the control performance of robotics actuators. In: Proc. 2007 IEEE/RSJ International Conference on Intelligent Robots and Systems, San Diego, CA, USA, pp. 1085–1092 (2007)

Jia-Fan, Z., Can-Jun, Y., Ying, C., Yu, Z., Yi-Ming, D.: Modeling and control of a curved pneumatic muscle actuator for wearable elbow exoskeleton. Mechatronics 18, 448–457 (2008)

Johansson, R.S., Birznieks, I.: First spikes in ensembles of human tactile afferents code complex spatial fingertip events. Nature Neuroscience 7(2), 170–177 (2004)

Johnson, K.O., Lamb, G.D.: Neural mechanisms of spatial tactile discrimination: Neural patterns evoked by Braille-like dot patterns in the monkey. J. Physiol. 310, 117–144 (1981)

Johnson, K.O., Phillips, J.R.: A rotating drum stimulator for scanning embossed patterns and textures across the skin. J. Neurosci. Methods 22, 221–231 (1988)

Johnson, K.O., Yoshioka, T.: Neural mechanisms of tactile form and texture perception. In: Nelson, R.J. (ed.) The Somatosensory System: Deciphering the Brain's Own Body Image, pp. 73–101. CRC Press LLC, Boca Raton (2001)

Jones, L.A., Lederman, S.J.: Tactile sensing. In: Jones, L.A., Lederman, S.J. (eds.) Human Hand Function, pp. 44–74. Oxford University Press, New York (2006)

Jutras, D., Bigras, P.: Control of an actuator made of two antagonist McKibben muscles via LMI optimization. In: Proceedings of the IEEE International Symposium on Industrial Electronic, pp. 3072–3077 (2006)

Kapandji, A.: The physiology of the joints – upper limb. Churchill Living-stone, Edinburgh (1982)

Kawamoto, H., Sankai, Y.: Power assist method based on phase sequence and muscle force condition for HAL. Advanced Robotics 19(7), 717–734 (2005)

Kiguchi, K., Tanaka, T., Fukuda, T.: Neuro-fuzzy control of a robotic exoskeleton with EMG signals. IEEE Transactions on Fuzzy Systems 12(4), 481–490 (2004)

Killebrew, J.H., Bensmaia, S.J., Dammann, J.F., Denchev, P., Hsiao, S.S., Craig, J.C., Johnson, K.O.: A dense array stimulator to generate arbitrary spatio-temporal tactile stimuli. J. Neurosci. Methods 161, 62–74 (2007)

Koganezawa, K., Ianba, T., Nakazawa, T.: Stiffness and Angle Control of Antagonistically Driven Joint. In: Proceedings of the IEEE International Conference on Biomedical Robotics and Biomechatronics, pp. 1007–1013 (2006)

Krebs, H.I., Hogan, N., Aisen, M.L., Volpe, B.T.: Robot-Aided Neurorehabilitation. IEEE Transactions on Rehabilitation Engineering 6(1), 75–87 (1998)

Kwakkel, G., Wagenaar, R.C., Twisk, J.W., Lankhorst, G.J., Koetsier, J.C.: Intensity of leg and arm training after primary middle-cerebral-artery stroke: a randomized trial. Lancet 354(9174), 191–196 (1999)

Kyung, K.U., Ahn, M., Kwon, D.S., Srinivasan, M.A.: A compact planar distributed tactile display and effects of frequency on texture judgment. Advanced Robotics 20, 563–580 (2006)

LaMotte, R.H., Friedman, R.M., Lu, C., Khalsa, P.S., Srnivasan, M.A.: Raised object on a planar surface stroked across the fingerpad: responses of cutaneous mechanoreceptors to shape and orientation. J. Neurophysiol. 80, 2446–2466 (1998)

LaMotte, R.H., Whitehouse, G.M., Robinson, C.J., Davis, F.: A tactile stimulator for controlled movements of textured surfaces across the skin. J. Electrophysiol. Tech. 10, 1–17 (1983)

Lauer, R.T., Peckham, P.H., Kilgore, K.L., Heetderks, W.J.: Applications of cortical signals to neuroprosthetic control: a critical review. IEEE Trans. Rehabil. Eng. 8, 205–208 (2000)

Lawrence, M.A., Kitada, R., Klatzky, R.L., Lederman, S.J.: Haptic roughness perception of linear gratings via bare finger or rigid probe. Perception 36, 547–557 (2007)

Lederman, S.J.: The perception of surface roughness by active and passive touch. Bulletin of the Phychonomic Society 18(5), 253–255 (1981)

Lenzi, T., De Rossi, S.M.M., Vitiello, N., Carrozza, M.C.: Proportional EMG control for upper-limb powered exoskeletons. In: Proc. of the 2011 Annual International Conference of the IEEE Engineering in Medicine and Biology Society (EMBC), Boston, USA, pp. 628–631 (2011)

Lenzi, T., De Rossi, S.M.M., Vitiello, N., Carrozza, M.C.: Intention-based EMG Control for Powered Exoskeletons. IEEE Transactions on Biomedical Engineering 59(8), 2180–2190 (2012)

Lenzi, T., De Rossi, S.M.M., Vitiello, N., Chiri, A., Roccella, S., Giovacchini, F., Vecchi, F., Carrozza, M.C.: The neuro-robotics paradigm: NEURARM, NEUROExos, HANDEXOS. In: Proc. of the International Conference of the IEEE Engineering in Medicine and Biology Society (EMBC 2009), Minneapolis, US, pp. 2430–2433 (2009)

Lenzi, T., Vitiello, N., De Rossi, S.M.M., Persichetti, A., GiovacchiniF, R.S., Vecchi, F., Carrozza, M.C.: Measuring Human-Robot Interaction on Wearable Robots: a Distributed Approach. Mechatronics 21(6), 1123–1131 (2011)

Lenzi, T., Vitiello, N., De Rossi, S.M.M., Roccella, S., Vecchi, F., Carrozza, M.C.: NEUROExos: A variable impedance powered elbow exoskeleton. In: Proc. of the 2011 IEEE International Conference on Robotics and Automation (ICRA), Shanghai, China, pp. 1419–1426 (2011)

Lenzi, T., Vitiello, N., McIntyre, J., Roccella, S., Carrozza, M.C.: A robotic model to investigate the human motor control. Biological Cybernetics 105(1), 1–19 (2011)

Libouton, X., Barbier, O., Plaghki, L., Thonnard, J.-L.: Tactile roughness discrimination threshold is unrelated to tactile spatial acuity. Behav. Brain Res. 208(2), 473–478 (2010)

Loizou, P.: Introduction to cochlear implants. IEEE Eng. Med. Biol. Mag. 18(1), 32–42 (1999)

Looft, F.J., Williams, W.J.: On-line receptive field mapping of cutaneous receptors. IEEE Trans. Biomed. Eng. 26, 350–356 (1979)

Lum, P.S., Burgar, C.G., Kenney, D.E., Machiel Van der Loos, H.F.: Quantification of Force Abnormalities During Passive and Active-Assisted Upper-Limb Reaching Movements in Post-Stroke Hemiparesis. IEEE Transactions on Biomedical Engineering 46(6), 652–662 (1999)

Manfredi, L., Assaf, T., Mintchev, S., Marrazza, S., Capantini, L., Orofino, S., AscariL, G.S., Wallén, P., Ekeberg, O., Stefanini, C., Dario, P.: A bioinspired autonomous swim-ming robot as a tool for studying goal-directed locomotion. Biological Cybernetics 107(5), 513–527 (2013)

Marsot-Dupuch, K., Meyer, B.: Cochlear implant assessment: imaging issues. European Journal of Radiology 40, 119–132 (2001)

Mayhew, D., Bachrach, B., Rymer, W., Beer, R.: Development of the MACARM-a Novel Cable Robot for upper Limb Neurorehabilitation. In: Proc. of the IEEE International Conference on Rehabilitation Robotics, Chicago, US, pp. 299–302 (2005)

Mertz, L.: The Next Generation of Exoskeletons: Lighter, Cheaper Devices Are in the Works. IEEE Pulse 3(4), 56–61 (2012)

Micera, S., Carrozza, M.C., Guglielmelli, E., Cappiello, G., Zaccone, F., Freschi, C., Colombo, R., Mazzone, A., Del Conte, C., Pisano, F., Minuto, G., Dario, P.: A Simple Robotic System for Neurorehabilitation. Autonomous Robots 19(3), 271–284 (2006)

Migliore, S.A., Brown, E.A., DeWeerth, S.P.: Biologically inspired joint stiffness control. In: Proceedings of the IEEE international Conference on Robotics and Automation, pp. 4508–4513 (2005)

Mihelj, M., Nef, T., Riener, R.: ARMin II – 7 DoF rehabilitation: mechanics and kinematics. In: Proc. of IEEE International Conference on Robotics and Automation (ICRA), pp. 4120–4125 (2007)

Muhammad, H.B., Recchiuto, C., Oddo, C.M., Beccai, L., Anthony, C.J., Adams, M.J., Carrozza, M.C., Ward, M.C.L.: A capacitive tactile sensor array for surface texture discrimination. Microelectron. Eng. 88, 1811–1813 (2011)

Mussa-Ivaldi, F.A., Hogan, N., Bizzi, E.: Neural, mechanical, and geometric factors subserving arm posture in humans. The Journal of Neuroscience 5, 2732–2743 (1985)

Nakazawa, N., Ikeura, R., Inooka, H.: Characteristics of human fingertips in the shearing direction. Biol. Cybern. 82(3), 207–214 (2000)

Nef, T., Mihelj, M., Riener, R.: ARMin: A robot for patient-cooperative arm therapy. Medical and Biological Engineering and Computing 45(9), 887–900 (2007)

Oddo, C.M., Beccai, L., Felder, M., Giovacchini, F., Carrozza, M.C.: Artificial roughness encoding with a bio-inspired MEMS-based tactile sensor array. Sensors 9, 3161–3183 (2009)

Oddo, C.M., Beccai, L., Muscolo, G.G., Carrozza, M.C.: A biomimetic MEMS-based tactile sensor array with fingerprints integrated in a robotic fingertip for artificial roughness encoding. In: Proc. 2009 IEEE Conference on Robotics and Biomimetics, Guilin, China, pp. 894–900 (2009)

Oddo, C.M., Beccai, L., Vitiello, N., Backlund Wasling, H., Wessberg, J., Carrozza, M.C.: A Mechatronic Platform for Human Touch Studies. Mechatronics 21, 604–613 (2011)

Oddo, C.M., Beccai, L., Wessberg, J., Backlund Wasling, H., Mattioli, F., Carrozza, M.C.: Roughness encoding in human and biomimetic artificial touch: spatiotemporal frequency modulation and structural anisotropy of fingerprints. Sensors 11, 5596–5615 (2011)

Oddo, C.M., Controzzi, M., Beccai, L., Cipriani, C., Carrozza, M.C.: Roughness Encoding for Discrimination of Surfaces in Artificial Active Touch. IEEE Trans. Robot. 27(3), 522–533 (2011)

Pasquero, J., Luk, J., Lévesque, V., Wang, Q., Hayward, V., MacLean, K.E.: Haptically enabled handheld information display with distributed tactile transducer. IEEE Trans. Multimedia 9(4), 746–753 (2007)

Pawluk, D.T.V., Howe, R.D.: Dynamic lumped element response of the human fingerpad. J. Biomech. Eng. 121, 178–183 (1999)

Perry, J.C., Rosen, J., Burns, S.: Upper-Limb Powered Exoskeleton Design. IEEE/ASME Transactions on Mechatronics 12(4), 408–417 (2007)

Pfeifer, R., Iida, F., Bongard, J.: New robotics: design principles for intelligent systems. Artif. Life 11, 99–120 (2005)

Polit, A., Bizzi, E.: Characteristics of motor programs underlying arm movements in monkeys. J. Neurophysiol. 42, 183–194 (1979)

Pons, J.L.: Wearable Robotics: Biomechatronic Exoskeletons. Wiley, New York (2008)

Pons, J.L.: Rehabilitation exoskeletal robotics. The promise of an emerging field. IEEE Engineering in Medicine and Biology Magazine 29, 57–63 (2010)

Popovic, D., Sinkjaer, T.: Control of movement for the physically disabled. Springer (2000)

Potkonjak, V., Popovic, M., Lazarevic, M., Sinanovic, J.: Redundancy Problem in Writing: From Human to Anthropomorphic Robot Arm. IEEE Transactions on Systems, Man, And Cybernetics-Part B: Cybernetics 28(6), 790–805 (1998)

Pratt, G., Williamson, M.M.: Series elastic actuators. In: Proceedings of the IEEE International Conference on Intelligent Robot and Systems, pp. 339–406 (1995)

Prescott, T.: Vibrissal behaviour in rodents and marsupials. Lecture at the Theo Murphy meeting on Active Touch Sensing. Chicheley Hall, Buckinghamshire (January 31, 2011)

Radwin, R., Jeng, O., Gisske, E.: A new automated tactility test instrument for evaluating hand sensory function. IEEE Transactions on Rehabilitation Engineering 1, 220–225 (1993)

Reinkensmeyer, D.J., Takahashi, C.D., Timoszyk, W.K., Reinkensmeyer, A.N., Kahn, L.E.: Design of robot assistance for arm movement therapy following stroke. Advanced Robotics 14(7), 625–637 (2001)

Rocon, E., Belda-Lois, J.M., Ruiz, A.F., Manto, M., Moreno, J.C., Pons, J.L.: Design and Validation of a Rehabilitation Robotic Exoskeleton for Tremor Assessment and Suppression. IEEE Transactions on Neural Systems and Rehabilitation Engineering 15(3), 367–378 (2007)

Romo, R., Ruiz, S., Crespo, P., Hsiao, S.S.: A tactile stimulator for studying motion processing in the somatic sensory system of primates. J. Neurosci. Methods 46, 139–146 (1993)

Ronsse, R., Vitiello, N., Lenzi, T., van den Kieboom, J., Carrozza, M.C., Ijspeert, A.J.: Human-robot synchrony: flexible assistance using adaptive oscillator. IEEE Transactions on Biomedical Engineering 58(4), 1001–1012 (2011)

Ronsse, R., Vitiello, N., Lenzi, T., van den Kieboom, J., Carrozza, M.C., Ijspeert, A.J.: Adaptive oscillators with human-in-the-Loop: Proof of concept for assistance and rehabilitation. In: Proc. of the 2010 3rd IEEE RAS and EMBS International Conference on Biomedical Robotics and Biomechatronics (BIOROB), Tokyo, Japan, pp. 668–674 (2010)

Sanchez, R.J., Liu, J., Rao, S., Shah, P., Smith, R., Rahman, T., Cramer, S.C., Bobrow, J.E., Reinkensmeyer, D.J.: Automating Arm Movement Training Following Severe Stroke: Functional Exercises With Quantitative Feedback in a Gravity-Reduced Environment. IEEE Transactions on Neural Systems and Rehabilitation Engineering 14(3), 378–389 (2006)

Sanchez, R.J., Wolbrecht, E., Smith, R., Liu, J., Rao, S., Cramer, S., Rahman, T., Bobrow, J.E., Reinken-meyer, D.J.: A Pneumatic Robot for Re-Training Arm Movement after Stroke: Rationale and Mechanical Design. In: Proc. of the IEEE International Conference on Rehabilitation Robotics (ICORR), pp. 500–504 (2005)

Schaal, S., Sternad, D.: Origins and violations of the 2/3 power law in rhythmic three-dimensional arm movements. Exp. Brain Res. 136, 60–72 (2001)

Schiavi, R., Grioli, G., Sen, S., Bicchi, A.: VSA-II: a novel prototype of variable stiffness actuator for safe and performing robots interacting with humans. In: Proc. of the IEEE International Conference on Robotics and Automation, pp. 2171–2176 (2008)

Schiele, A., van der Helm, F.C.: Kinematic Design to Improve Ergonomics in Human Machine Interaction. IEEE Transaction on Neural Systems and Rehabilitation Engineering 14(4), 456–469 (2006)

Schneider, W., Slugg, R.M., Turnquist, B.P., Meyer, R.A., Campbell, J.N.: An electromechanical stimulator system for neurophysiological and psychophysical studies of pain. J. Neurosci. Methods 60, 61–68 (1995)

Serina, E.R., Mote, C.D., Rempel, D.: Force response of the fingertip pulp to repeated compression – effects of loading rate, loading angle and anthropometry. J. Biomech. 30(10), 1035–1040 (1997)

Simmons, F.B., Epley, J.M., Lummois, R.C.: Auditory nerve: electrical stimulation in man. Science 148, 104–106 (1965)

Smith, A.M., Chapman, C.E., Deslandes, M., Langlais, J.-S., Thibodeau, M.-P.: Role of friction and tangential force variation in the subjective scaling of tactile roughness. Exp. Brain Res. 144, 211–223 (2002)

Spelman, F.A.: The past, present, and future of cochlear prostheses. IEEE Eng. Med. Biol. Mag. 18(3), 27–33 (1999)

Spigler, G., Oddo, C.M., Carrozza, M.C.: Soft-neuromorphic artificial touch for applications in neuro-robotics. In: Proc. 2012 IEEE RAS/EMBS International Conference on Bio-Medical Robotics and Biomechatronics, Roma, Italy, pp. 1913–1918 (2012)

Stefanini, C., Orlandi, G., Menciassi, A., Ravier, Y., La Spina, G., Grillner, S., Dario, P.: A Mechanism for Biomimetic Actuation in Lamprey-like Robots. In: Proc. of the IEEE/RAS-EMBS International Conference on Biomedical Robotics and Biomechatronics, pp. 579–584 (2006)

Stein, R.B., Peckham, P.H., Popovic, D.P.: Neural prosthesis. Oxford University Press (1992)

Sternad, D., Schaal, S.: Segmentation of endpoint trajectories does not imply segmented control. Exp. Brain Res. 124, 118–136 (1999)

Stienen, A., Hekman, E., Van der Helm, F., Prange, G., Jannink, M., Aalsm, A., Van der Kooij, H.: Freebal: Dedicated gravity compensation for the upper extremities. In: Proc. of the International Conference on Rehabilitation Robotics, Noordwijk, The Netherlands, pp. 804–808 (2007)

Stienen, A., Hekman, E., Van Der Helm, F.T.H., Prange, G., Jannink, M., Aalsma, A., Van Der Kooij, H.: Dampace: dynamic force-coordination trainer for the upper extremities. In: Proc. IEEE 10th Int. Conf. Rehabi. Robot, Noordwijk, pp. 820–826 (2007)

Stienen, A.H.A., Hekman, E.E.G., ter Braak, H., Aalsma, A.M.M., van der Helm, F.C.T., van der Kooij, H.: Design of a rotational hydro-elastic actuator for a powered exoskeleton for up-per-limb rehabilitation. IEEE Transactions on Biomedical Engineering, accepted for future publication (2009)

Stienen, A.H.A., Hekman, E.E.G., van der Helm, F.C.T., van der Kooij, H.: Self-Aligning Exoskeleton Axes Trough Decoupling of Joint Rotations and Translations. IEEE Transactions on Robotics 25(3), 628–633 (2009)

Summers, I.R., Chanter, C.M.: A broadband tactile array on the fingertip. J. Acoust. Soc. Am. 112, 2118–2126 (2002)

Sup, F., Bohara, A., Goldfarb, M.: Design and Control of a Powered Transfemoral Prosthesis. The International Journal of Robotics Research 27(2), 263–273 (2008)

Tondu, B., Ippolito, S., Guiochet, J., Daidie: A Seven-degree-of-freedom Robot-arm Driven by Pneumatic Artificial Muscle for Humanoid Robots. The International Journal of Robotic Research 24(4), 257–274 (2005)

Tsagarakis, N.G., Caldwell, D.G.: Development and Control of a 'Soft-Actuated' Exo-skeleton for Use in Physiotherapy and Training. Autonomous Robots 15, 21–23 (2003)

Vallery, H., Veneman, J., Van Asseldonk, E., Ekkelenkamp, R., Buss, M., Van Der Kooij, H.: Compliant actuation of rehabilitation robots. IEEE Robot. Autom. Mag. 15(3), 60–69 (2008)

Van Damme, M., Verrelst, B., Van Ham, R., Daerden, F., Lefeber, D.: Proxy-based sliding mode control of a planar pneumatic manipulator. Int. J. Robot. Res. 28, 266–284 (2009)

Van Ham, R., Vanderborght, B., Van Damme, M., Verrelst, B., Lefeber, D.: MACCEPA, the mechanically adjustable compliance and controllable equilibrium position actuator: design and implementation in a biped robot. Robot. Auton. Syst. 55(10), 761–768 (2007)

Vanderborght, B., Van Ham, R., Lefeber, D., Sugar, T.G., Hollander, K.: Comparison of mechanical design and energy consumption of adaptable, passive-compliant actuators. Int. J. Robot. Res. 28, 90–103 (2009)

Velliste, M., Perel, S., Spalding, M.C., Whitford, A.S., Schwartz, A.B.: Cortical control of a prosthetic arm for self-feeding. Nature 453, 1098–1101 (2008)

Velliste, M., Perel, S., Spalding, M.C., Whitford, A.S., Schwartz, A.B.: Cortical control of a prosthetic arm for self-feeding. Nature 453(7198), 1098–1101 (2008)

Veneman, J.F., Ekkelenkamp, R., Kruidhof, R., van der Helm, F.C.T., van der Kooij, H.: A Series Elastic- and Bowden-Cable-Based Actuation of Use Torque Actuator in Exoskeleton-Type Robots. The International Journal of Robotics Research 25(3), 261–281 (2006)

Vidal-Verdú, F., Hafez, M.: Graphical tactile displays for visually-impaired people. IEEE Transactions on Neural Systems and Rehabilitation Engineering 15, 119–130 (2007)

Vitiello, N., Cattin, E., Roccella, S., Giovacchini, F., Vecchi, F., Carrozza, M.C., Dario, P.: The NEURARM towards a Platform for Joint Neuroscience on Human Motion Control Theories. In: Proc. of the 2007 IEEE International Conference on Intelligent Robots and Systems (IROS 2007), San Diego, CA, USA, pp. 1852–1857 (2007)

Vitiello, N., Lenzi, T., De Rossi, S.M.M., Roccella, S., Carrozza, M.C.: A sensorless torque control for Antagonistic Driven Compliant Joints. Mechatronics 20, 355–367 (2010)

Vitiello, N., Lenzi, T., McIntyre, J., Roccella, S., Cattin, E., Vecchi, F., Carrozza, M.C.: Charac-terization of the NEURARM bio-inspired joint position and stiffness open loop controller. In: Proc. of the 2008 IEEE International Conference on Biomedical Robotics and Biomechatronics (BIOROB 2008), Scottsdale, Az, USA, pp. 138–143 (2008)

Vitiello, N., Lenzi, T., Roccella, S., De Rossi, S.M.M., Cattin, E., Giovacchini, F., Vecchi, F., Carrozza, M.C.: NEUROExos: A Powered Elbow Exoskeleton of Physical Rehabilitation. IEEE Transactions on Robotics 29(1), 220–235 (2013)

Von Gierke, H.E., Keidel, W.D., Oestreicher, H.L.: AGARD Conference Proceedings 44: Principles and Practice of Bionics. In: AGARD Conference Proceedings, Slough, U.K., vol. 44, pp. 371–387 (1970)

Wagner, C.R., Lederman, S.J., Howe, R.D.: A tactile shape display using RC Servomotors. In: Proc. 2002 IEEE Symposium on Haptic Interfaces for Virtual Environment and Teleoperator Systems, Orlando, USA, pp. 354–355 (2002)

Wheat, H.E., Salo, L.M., Goodwin, A.W.: Human ability to scale and discriminate forces typical of those occurring during grasp and manipulation. J. Neurosci. 24, 3394–3401 (2004)

Wolpert, D.M., Ghahramani, Z., Jordan, M.I.: An Internal Model for sensorimotor integration. Science 269(5232), 1880–1882 (1995)

Wolpert, D.M., Miall, R.C., Kawato, M.: Internal models in the cerebellum. Trends in Cognitive Sciences 2(9), 338–347 (1999)

Yoshioka, T., Gibb, B., Dorsch, A.K., Hsiao, S.S., Johnson, K.O.: Neural coding mechanisms underlying perceived roughness of finely textured surfaces. J. Neurosci. 21, 6905–6916 (2001)

Zollo, L., Eskiizmirliler, S., Teti, G., Laschi, C., Burnod, Y., Guglielmelli, E., Maier, M.A.: An anthropomorphic Robotic Platform for Progressive and Adaptive Sensorimotor Learning. Advanced Robotics 22, 91–118 (2008)